Imperial College London

FYP - Experimental Assessment of Fast Charging Techniques in Lithium-Ion Batteries

-

Can constant-temperature charging strategies be combined with additional existing strategies to reduce cell degradation?

Final Report

4th June 2020

Jake Reynolds

Department of Mechanical Engineering

Supervisor: Dr Monica Marinescu

Associate Supervisor: Dr Laura Bravo Diaz

Keywords: Electric Vehicle, Lithium-ion Battery, Charging Strategy, Constant-Temperature Charging, CC-CT-CV, SEI Formation

11999 / 12000

Acknowledgements

I would like to thank my supervisor, Dr Monica Marinescu, for the guidance and encouragement provided throughout this project. I would also like to thank my co-supervisor, Dr Laura Bravo Diaz for her time and support, particularly in the laboratory.

Despite interruptions caused by COVID-19, the Electrochemical Science and Engineering, ESE, Group at Imperial College London deemed this work to be "within probable sight of a publication" and allowed the project to continue. I would like to thank everyone involved in this decision, as well as the volunteers who have been visiting the laboratory to monitor and edit ongoing experiments; Alastair Hales, Niall Kirkaldy, Ryan Prosser, Oisin Shaw and Yan Zhao, thank you.

Abstract

The charging strategy used on a cell or battery pack can drastically affect its charge time and lifespan. This project aims to develop a novel charging strategy to improve upon existing techniques, with a focus on constant-temperature, CT, charging and electric vehicle industrial applications.

The only prior study on CT strategies achieved a reduction in the rise of the cell's surface temperature by 20% when compared to a CC-CV charge of identical charge time. It is suggested that this reduction in temperature would result in less degradation, in turn leading to a longer cell life. The maximum current, however, was doubled to achieve this. Modelling predictions made during this project using LIONSIMBA suggest that similar results can be achieved without the use of excessive currents by using a constant-current, CC, stage to begin the charge.

This novel CC-CT-CV strategy is tested against a control CC-CV strategy on two LGM50 21700 cells. A reduction in charge time of 7.4% is achieved whilst the temperature rise is simultaneously reduced by 28.7%. Degradation tests, (namely pulse testing, open circuit voltage tests and incremental capacity analysis), confirm that this strategy will results in less degradation, with capacity fade and ohmic resistance increase reducing by 24.8% and 45% respectively.

These results suggest that there is great potential for CT charging strategies, specifically CC-CT-CV, and it is hoped that this work will impact on the methods used to charge electric vehicles in future.

Contents

1. Introduction

This project aims to develop a novel charging strategy, with a focus on constant temperature, CT, charging, a concept which has only recently been considered by researchers (1). It builds upon the work of Patnaik et al. (1), who reported the first successful use of CT charging in 2019, as well as a literature review on charging strategies (2), which concluded that CT charging strategies are a promising new technology.

1.1 Motivation

The motivation for this research is threefold and is provided in this section. First, the drive to study, develop and manufacture technologies for electric vehicles, EVs, is outlined. Second, the specific choice of technology, charging strategies, is justified. Finally, the decision to focus on the yet more niche field of CT charging is explained.

Transport linked CO_2 emissions increased by 2.5% annually between 2010 and 2015, accounting for a 23% share of global energy related CO_2 emissions (3). For the UK to meet its target of net zero CO_2 emissions, it is imperative that the government adheres to its mandate of electrification of commercial vehicles by the year 2050 (4). Driven by these government commitments, combined with the ability to mass manufacture suitable technologies and investments made in field over the last 20 years, (5), there has been growing commercial and consumer interest in EVs. The general population's concern for the environment has also gown, and a gradual shift in opinion now means that the public not only *need* EVs, but they *want* them. This growing demand has led to an associated boom in the requirement to improve EV technologies and therefore, an increase in battery research in general.

-

The range an EV can achieve has increased drastically in recent years, (6). As a result, they now provide a viable alternative to combustion powered vehicles. (7). Despite this, EVs still face a multitude of challenges. These include, but are not limited to, infrastructure development, charge time and lifespan. The latter two inspired this project, with the ambition being to contribute to research into improving charge time and/or decreasing the degradation of a battery pack (8).

There are a wide range of solutions currently being investigated, from dielectric cooling systems, (9), to tab cooling (10). Entirely novel technologies are also being explored, from supercapacitors to solid state batteries, (where the focus is primarily on safety), (11). The motivation to study charging strategies, a perhaps underrated technology, instead of these more well-known and 'glamorous' ideas is highlighted below.

First, whilst a new technology can be promising in a laboratory, it is often an expensive and time-consuming challenge to mass produce it. This is particularly clear for solid-state batteries, and the financial struggle can be seen when looking at the recent failures of Dyson Technologies' EV (12).

Second, some developments maybe relatively simple to mass manufacture when they are viewed as a separate system to the EV, however, integrating the technology may cause additional and unforeseen complications. An example of this is some of the liquid cooling technologies being developed. Results may show promising improvements when a pack is cycled in the laboratory, however the resulting benefits may be countered by the additional weight added to the vehicle (9).

Third, whilst a novel technology maybe promising in one area, it may fall short in other crucial aspect. An obvious suspect of this is supercapacitors. They may offer immense charging speeds; however, their energy density is currently too low to achieve the ranges required and, more importantly, expected, in the commercial vehicle industry.

An entire Literature Review, or indeed FYP, could be conducted to discuss which technology, or technologies combined, should be prioritised. Broadly speaking, however, the critical state of our planet's environment means that we cannot wait for entirely new solutions to come to fruition. Instead, or at least in parallel, we must explore how improvements to *existing* charging strategies can quickly be used to improve *existing* EV technology.

-

CT charging is a form of closed-loop charging, the details of which will be discussed in the literature review. In general, live measurements from the cell are used to adjust the current to maintain a constant temperature. As discussed in the 'Project Plan', these strategies have been found to improve charging speeds by 20% whilst maintaining the same surface temperature across the cell when compared to constant-current constant-voltage, CC-CV, charging (1). This project looks to further improve on these CT charging strategies (13). To date, only one paper has been published which considers and experiments with CT charging, and the results are promising. There is currently no work which discredits the idea (2), and there is a clear opportunity to improve EV technology by studying CT charging in more detail.

1.2 Objectives

Initially, the objective of this project was to ascertain if CT charging strategies can improve upon existing charging strategies. The initial research question was:

Can constant-temperature charging strategies be combined with additional existing strategies to reduce cell degradation?

Through researching literature and modelling predictions, a specific novel charging strategy was developed whereby the cell is charged with a constant-current, CC, before entering a CT stage, and finally ending with a traditional constant-voltage, CV, charge. The name CC-CT-CV was coined, and the research question was updated to:

Can constant-temperature charging strategies be further improved by introducing an initial CC stage to reduce the maximum current whilst maintaining the benefits in charge time?

This project has a strong focus on industrial application. To reflect this, the cells have been selected to mirror EV development, specifically 21700s (LGM50s), and any charging strategies developed must be applicable in this industry (13). During this project, Tesla announced a partnership with LG Chem specifically for these cells, making this selection even more relevant (7).

This project aims to add further evidence that CT charging is beneficial for the cell, in the form of the first degradation study to occur on this strategy. The study is specifically on a novel type of CT charging, the CC-CT-CV charging strategy. These aims, as well as additional points, are summarised in a list of key objectives below (8).

- Add to the battery model LIONSIMBA such that it can run closed-loop charging strategies.
- Test numerous CT profiles using LIONSIMBA and select the 'most promising' to experiment with.
- Physically recreate the CT profile such that it can be cycled on a cell.
- Perform characterisation tests to determine if the profile would increase cell life while simultaneously improving charge time and temperature rise, ΔT, (this would be the first degradation study on any CT charging strategy).

2. Literature Review

The research presented below is intended to be specific to cylindrical lithium-ion cells, however, in places, it can be applied to a more general range of cells. The very basics of battery operation are omitted here (14); instead the focus will be on degradation and the specifics of charging strategies.

2.1 Degradation Mechanisms

There are many processes occurring within a cell which, overtime, lead to a loss of power, capacity and ultimately, the failure of the cell (15). These are called degradation mechanisms. Figure 1, (15) shows a wide range of degradation mechanisms which take place inside the cell. This section will discuss the details of two, lithium plating, Li-plating, and solid electrolyte interphase, SEI, growth, as well as the causes of many others.

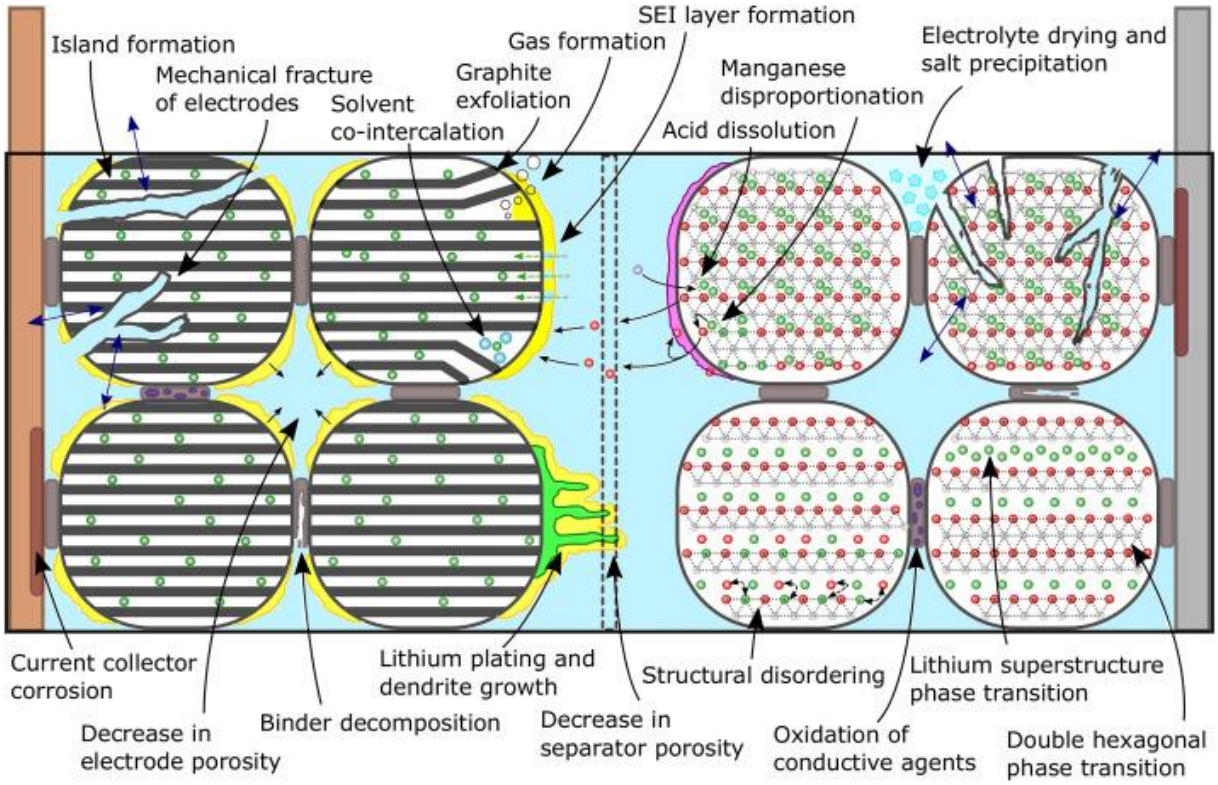

Figure 1 - Degradation mechanisms occurring within a Li^+ cell - (15) p.4

-

Li-plating, shown in green in Figure 1, occurs predominantly during charging whilst lithium-ions, (Li^+), are arriving at the anode (2). Instead of the usual process of intercalation with the carbon, the Li^+ are reduced, forming lithium metal at the surface. These Li^+ are effectively used up, resulting in a loss of capacity and,

therefore, a reduction in the cycle life. Further, the thickness of the lithium metal can continue to grow with additional plating and dendrite growth can occur, leading to a piercing of the separator and, consequently, a short circuit, rendering the cell useless (16).

The longest step in battery operation is the intercalation of the Li^+ into the anode. If the transfer of these ions from the cathode is significantly faster than the intercalation, there will be a build up at the surface of the anode which leads to Li-plating This is often caused by high currents occurring at high states of charge, SOCs, and is a key reason a constant-voltage, CV, charging stage is used to end most charging strategies (16), (17).

The operating temperature of the cell will affect the rate of transfer of ions, as well as the intercalation speed, and will therefore have a direct effect on Li-plating. As with most aspects of battery modelling, there are many models to describe Li-plating (18). Having said this, most of these models, which are supported by experimental evidence, agree that that Li-plating's dependency on temperature is analogous to an Arrhenius law (19), as shown by Equation 1 (20):

$$X_T = X_0 \, exp\left[\frac{E_{a,x}}{R}\left(\frac{1}{T_0} - \frac{1}{T}\right)\right] \tag{1}$$

Where $\boldsymbol{X}$ refers to all temperature dependant terms within a greater model which will be proportional to the rate of Li-plating, ($\boldsymbol{X_0}$ and $\boldsymbol{X_T}$ refer to X at some reference temperature $\boldsymbol{T_0}$ and some other temperature $\boldsymbol{T}$ respectively). $\boldsymbol{E_{a,x}}$ represents the activation energy for the term $\boldsymbol{X}$, and $\boldsymbol{R}$, some constant.

Equation 1 clearly shows an inverse relationship between temperature and Li-plating; charging at lower temperatures results in more Li-plating and therefore, when viewed in isolation, greater amounts of capacity fade (2).

-

Another common type of degradation found within cells is the formation of the SEI, shown in yellow in Figure 1. As will be shown here, the dependency on temperature is opposite to that of Li-plating, which results in a delicate balance between the two mechanisms.

Whilst SEI formation is usually referred to as a degradation mechanism, it is important to note that its existence is vital to the function of a battery (21), (it acts as an electron insulating barrier between the electrodes and the electrolyte). Any attempts to prevent its growth must not, therefore, prevent it from forming.

Under certain conditions, the Li^+ arriving at the anode do not intercalate, nor do they contribute to Li-plating. Instead, these ions react with organic compounds contained within the electrolyte to form a complex solid around the electrode (22). This solid is called the SEI; a schematic of its formation is provided in Figure 2. The highly reactive lithium metal formed during Li-plating can also react with these organic compounds, further adding to SEI growth (17), (23), (this would not reduce capacity any more than the Li-plating already had). In total, SEI growth leads to capacity losses varying from 10 to 100% during a cell's lifetime (24).

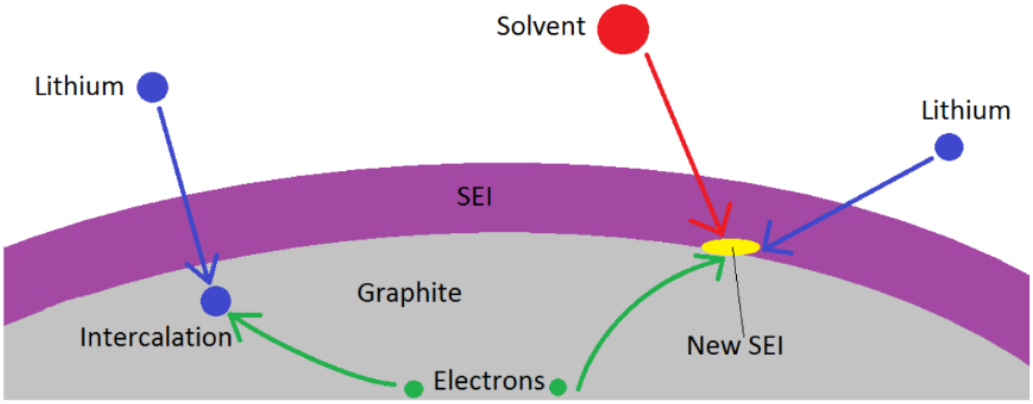

Figure 2 - Schematic of SEI formation - (22) p.4

As with Li-plating, there is no one true model for SEI growth. A comprehensive study of accepted models is, however, provided by Pinson et al. (25). They show that there is again a relationship with the Arrhenius law, caused by the diffusion of Li^+ (2). Unlike Li-plating however, the rate of SEI growth is directly proportional to temperature. Pinson et al. also show that higher C-rates lead to an acceleration in growth, as an increase in current leads to an increase in heat generation, see section 2.3.

Any charging strategy that could maintain the temperature of the cell at a constant, optimal level could be used to manage these degradation mechanisms.

-

Having discussed the two most notorious degradation mechanism, it is worth briefly considering other mechanisms, specifically, their relationships to temperature and voltage. It is also worth noting that degradation mechanisms are not independent (26). Perhaps the clearest example of this SEI growth and decomposition of the electrolyte.

Table 1, (27), shows several degradation mechanisms and their dependency to cell temperature and voltage.

Table 1 - A range of degradation mechanisms, their locations and dependencies

Mechanism	Location	Worse when Temp:	Other Relationships Worse at:
SEI	Anode	High	High SOCs
Li-Plating		Low	High voltages and SOCs
Graphite Exfoliation & Cracking		High	-
Structural Disordering	Cathode	Low	-
Metal Dissolution		High	High or low voltages
Cathode Film Formation			High voltages
Phase Transitions			-
Electrode Fracture	Electrodes		-
Binder Decomposition			-
Current Collector Corrosion			High voltages
Oxidation of Conductive Material			
Electrolyte Drying	Throughout		

These mechanisms all have some relationship with temperature, whilst not all have a relationship with voltage. It is perhaps peculiar that previous charging strategies have only considered voltage control, and not temperature control or, at least, some combination of both.

2.2 Degradation Measures

The techniques used to measure degradation used in this study are ex-situ, non-destructive techniques (28), allowing the cell to be continued to be cycled after it has been characterised. The nuances of an open circuit voltage test, OCV, pulse testing and incremental capacity analysis, ICA, are all briefly discussed here.

-

Equation 2 shows how the voltage of a cell depends on the OCV, as well as a current based term (29).

$$V_{cell} = IR_{losses} + OCV \tag{2}$$

By charging/discharging the cell with a low current, C/24, the first term becomes negligible and the OCV of the cell can be obtained. Charging at this current ensures that all the available lithium has had time to diffuse into the electrode, meaning that the total available capacity can be found. Coulomb counting,

effectively numerical integration, is applied to the current with respect to time to obtain the true capacity of the cell (29).

-

Pulse testing fits experimental data, specifically the voltage sag after a current is applied, to an equivalent circuit model, ECN of a cell. Here, a first order ECN model is used as shown in Figure 3.

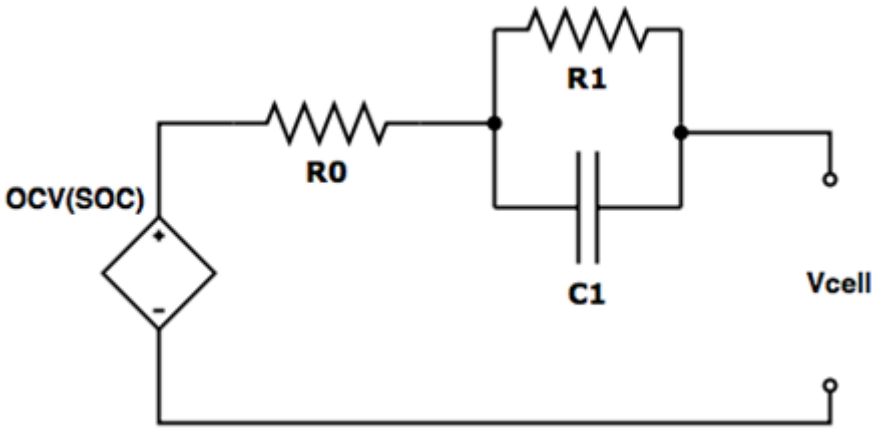

Figure 3 - First order ECN model of a lithium-ion cell - (30) p.11

R_0 models the series, or ohmic, resistance of all cell components. This includes, but is not limited to, the electrolyte, electrodes, contact resistances, and the SEI. The change in this resistance therefore provides insight into the amount of degradation that has taken place within the cell (31). The physical representation of R_1, or lumped resistance, is perhaps more complicated. As shown by Figure 4, it models the transient behaviour of the cell, including the charge transfer resistance.

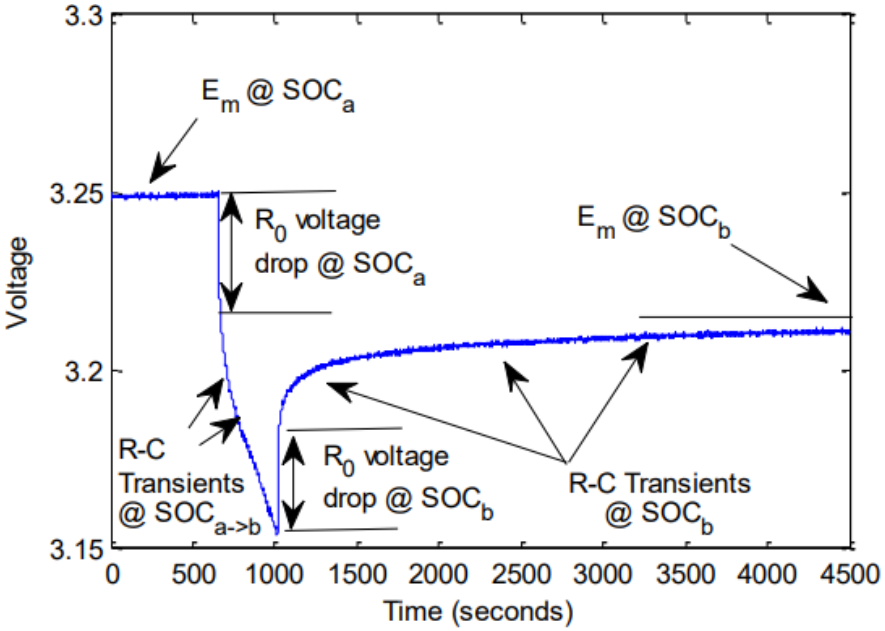

Figure 4 - Voltage sag labelled with links to the ECN - (31) p.3

It should be noted that pulse testing was performed with relatively short rest times and, therefore, contributions from slow processes might not be reflected, i.e. R_1 may be underestimated. Similarly, despite using a high sampling rate, see section 4.3, R_0 could be overestimated as it represents the instantaneous response, occurring in the order of milliseconds.

-

Neither pulse testing, nor OCV tests, can clearly distinguish between different types of degradation. ICA, however, does however usually allow some identifications to be made. As the data collected for an OCV test is identical to the data required to perform ICA, (with some additional data processing necessary), it was decided that this technique would also be used.

Traditionally by initially filtering the data, ICA transforms plateaus occurring on the OCV voltage/capacity plots to peaks on a $\frac{dQ}{dV}$ vs voltage plot, or incremental capacity, IC, curve (32). Many papers show how these peaks each refer to different degradation mechanisms; however, the position and movement of these peaks depends greatly on the cell chemistry (33).

Further, the results depend on the filtering technique used when processing the data, making it difficult to compare across studies. A novel method, called the LEAN method, was recently suggested to remove this issue (34), however it was not implemented in this study due to time constraints.

2.3 Heat Generation

Having understood the degradation mechanisms which lead to a reduction in cell life, and recognising these processes' high dependence on temperature, it is important to grasp what factors cause a cell to generate heat. A brief overview is provided here.

The heat generation that occurs in lithium-ion cells can be split into two categories; reversible and irreversible heat generation (35). Reversible heat generation, also known as entropic heat generation, is a consequence of the exothermic or endothermic reactions that occur during phase changes of the materials within the cell. Irreversible heat generation can be split into two categories, ohmic heating, (caused by the resistances associated with limitations to current flow), and kinetic heating, (related to charge transfer reactions at the electrode-electrolyte interfaces), (36).

The following, simplified, equation was obtained from fundamental thermodynamic principles by Bernardi et al. (37), and is now commonly cited in battery literature.

$$\dot{Q}_{gen} = R_{int} \cdot I^2 - I \cdot \left(T_{cell} \cdot \frac{dU_{OC}}{dT} \right) \quad (3)$$

The first and second terms represent the irreversible and reversible heat generation respectively.

It has been previously shown that an increase in temperature can lead to an increase in resistance, (through degradation mechanisms such as SEI growth). Equation 3 shows how this increase in resistance will lead to additional heat generation in future cycles. Heat generation will also be caused by a higher current.

-

The purpose of these sections has not been to explain the exact relationships between the rate of degradation, cell temperature and internal resistance. This research, however, does show how dependent the operation of a cell or battery pack is on its temperature, and that it is hard to argue that controlling this temperature during charging would have anything other than a positive impact on the cell.

2.4 Charging Strategies

There are variety of solutions used to reduce cell degradation and/or increase charging speed. Multiple charging strategies will be discussed to understand existing techniques to improve cell life and charging speed and provide a reasonable comparison for the work presented in this report.

For clarification, the term 'current profile' is used when discussing a particular input current which could be drawn on a Current/Time graph, whilst 'charging strategy' is used when referring to a collective group of current profiles, for example, all CC-CV profiles.

Perhaps the most common charging strategy is CC-CV, which is used in applications from mobile phones to EVs, (38), (39). For this reason, CC-CV will be used as a control for both modelling and laboratory-based experiments. As the name suggests, this strategy begins by charging with CC, and, once the cell reaches a predetermined maximum voltage, $V_{max,}$ (most commonly 4.2V for Li^+ technologies (1)), ends with a CV charge, where the current will decay gradually. A general sketch of CC-CV is provided in Figure 5 (40).

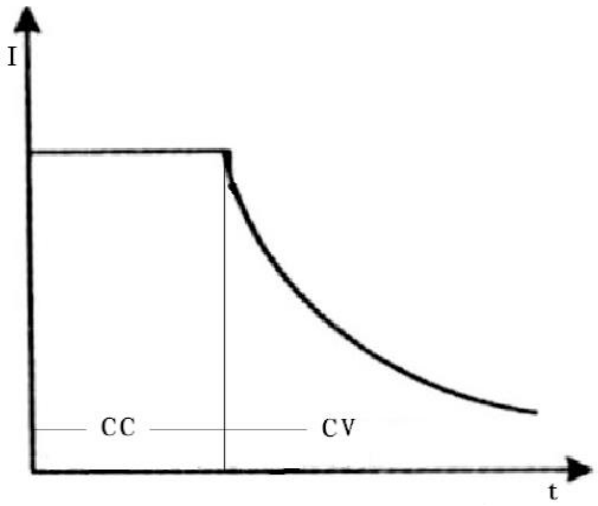

Figure 5 - Sketch of CC-CV charging - (40) p.1

The overarching idea of CC-CV charging is to avoid the high currents at high SOCs which can lead to Li-plating. The strategy helps combat the bottleneck build-up of Li^+ around the anode, with the CV stage allowing these ions to diffuse gradually into the electrode.

Whilst CC-CV charging is a simple method to fully and safely charge a cell, its capabilities regarding extending cell life are relatively limited (2). CC-CV has, albeit simple, control over the current and voltage passing though the cell and no direct control over the temperature of the cell.

It is worth noting that there is very little standardisation when it comes to comparing results of different papers and experiments (2). For example, Patnaik et al. report that CC-CV causes temperature rises from 3 to 7°C when charging occurs below 1C. This, already substantial, range would vary depending on, for example, the exact cell chemistry, cooling mechanism, ambient temperature and state of health of the cell. The inability to fairly compare the results of different profiles from different papers is a serious issue, perhaps even failure, of recent charging strategy research. For this reason, the precise performance, (in terms of ΔT, charge time and degradation), of CC-CV and other charging strategies are not discussed here. Any relevant and plausible comparisons with the novel charging strategy developed in this project

will be considered in the discussion, where comparisons will also be made with a cell which has undergone cycling with CC-CV under identical conditions.

Additional charging strategies have been developed, either as an extension to or novel combination of CC-CV, or as an entirely new concept. Figure 6 shows schematics of six, including CC-CV, of the most common strategies (41):

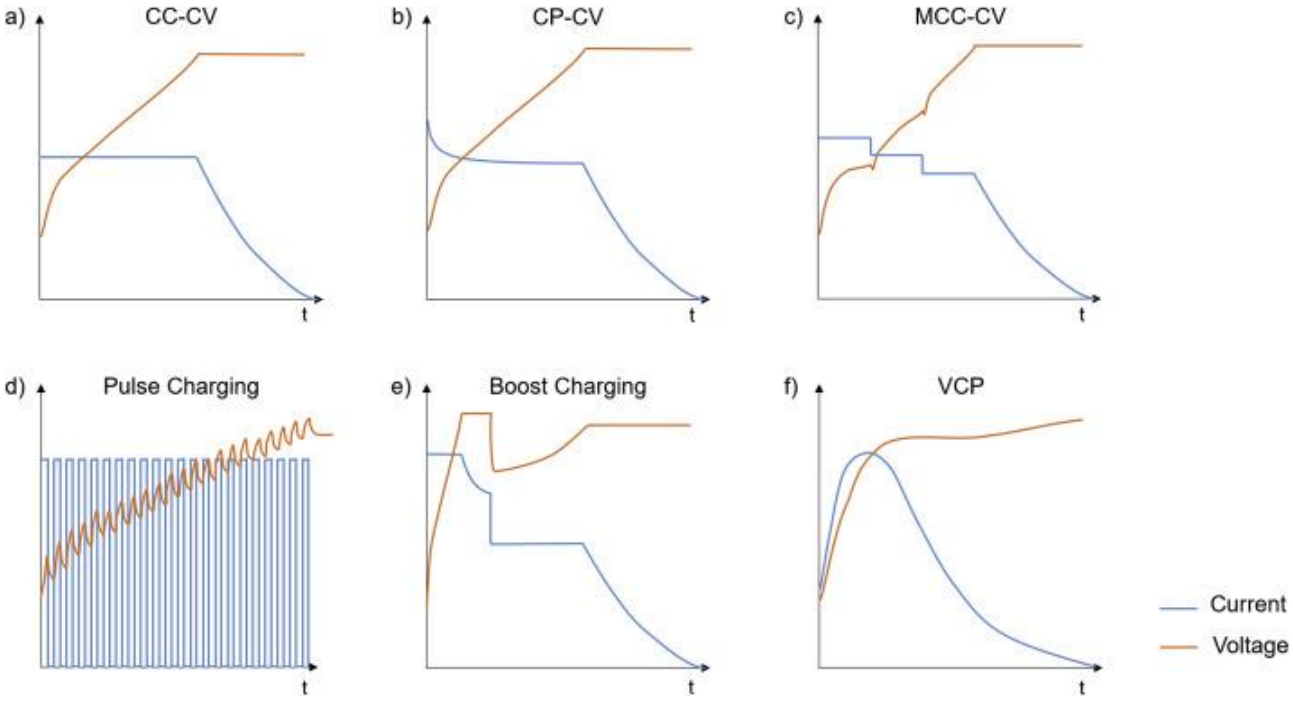

Figure 6 - Current/Time graphs of different strategies, often associated with fast charging. a) CC-CV, b) Constant-Power, Constant-Voltage, c) Multistage Constant-Current, Constant-Voltage (MCC-CV), d) Pulse charging, e) Boostcharging, f) Variable Current Profile - (41) p.14

It should be made clear that the aim of this project is to develop a strategy which causes less degradation, with the knowledge that the current could perhaps be increased to result in a faster charge for the same amount of degradation; more work, however, would be needed to confirm this.

2.6 Constant-Temperature Charging

It has been shown that there is a clear link between temperature and the lifespan of the cell, as well as the rate at which the cell is charged. This knowledge is not novel and has been around for almost as long as battery technology itself. The idea of charging at a constant temperature could perhaps be viewed as obvious, and anyone not fully versed in battery technology may presume that it is already adopted. In some senses, this is true. There are a whole host of battery cooling techniques in development, some of

which are already used in EVs, (9), (10), (42). These systems, however, add complexity, cost and weight to any battery pack that uses them. The novel version of CT is an entire charging strategy whereby the current is altered depending on the temperature of the cell, with the aim to maintain it at some optimum level.

The term 'constant-temperature charging' has been used for years in battery research fields; predominantly when referring to cooling of a cell or battery pack as explained above. In fact, this caused some confusion when discussing the project with members of the department. To clarify this point, the term 'constant-temperature' or 'CT' will be hereafter used to refer to this novel charging strategy, unless otherwise stated.

In 2019, Patnaik et al. published their paper which discussed and experimented with CT charging, specifically constant-temperature constant-voltage, CT-CV. It was the first investigation into any closed-loop charging technologies, one in which the charging input depends on some measured output. The profile was developed using proportional–integral–derivative, PID, control to maintain a constant temperature during the CT stage. Figure 7 shows the key results obtained by their experimentation, which was performed on an 18650 cylindrical Li^+ cell.

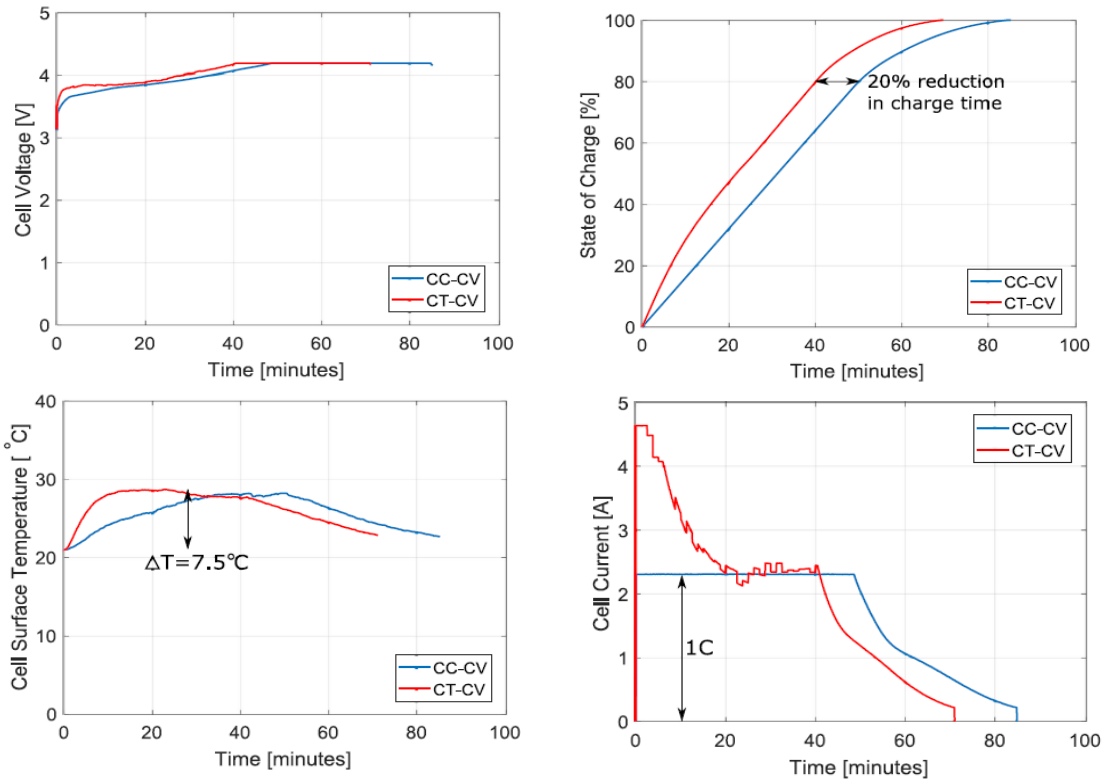

Figure 7 - Existing results from a CT charging strategy - (1) p.7

The study showed that CT charging was possible. Even more substantially, the results showed that a 20% reduction in charge time could be achieved for the same ΔT when compared to CC-CV. Alternatively, a 20% reduction in ΔT could be achieved for the same charge time.

-

This literature review helped develop the objectives outlined in the introduction and provided a clear connection between cell degradation and temperature. Perhaps the most substantial finding was the sheer lack of papers relating specifically to feedback-related CT charging. Whilst this means that there is currently very little evidence to support the benefits of CT charging, by definition, it also implies that there is nothing to suggest that it should not be an area for further consideration. This topic remains, therefore, a relatively novel and exciting area of research (13).

3. Modelling

It was decided that some computational modelling should be conducted before physical experimentation would begin. The predictions from the model would provide additional validity to the limited results in this field and narrow down ideas to be taken to the laboratory.

Up to this point, CT charging has been discussed as a general term. The details of how and why this method works have been presented, however, the ways in which CT charging can be applied have not. For example, CC charging can occur at multiple C-rate, in combination with copious other strategies, (e.g. CC-CV), and comes in many forms, (e.g. MCC). The same is true for CT charging; the only distinction is CC charging has been used for many years and there are, therefore, already many variations.

As will be shown in this section, the power of a model comes from the ability to perform many experiments in a relatively short period of time. The idea for the novel strategy that this project has produced was ultimately had whilst modelling, and this stage of the project is, therefore, much more significant than it was perhaps initially intended to be. The following section will outline the modelling methods used, as well as the key developments and findings.

It is important to note that the model setup, along with several findings, were completed before the progress report was submitted. Some text from the progress report has, therefore, been reused. Wherever this has occurred, the initial report has been clearly referenced.

3.1 Modelling Methods

The open source MATLAB based model 'LIONSIMBA' was chosen, in part due to its relative simplicity (13). LIONSIMBA is as pseudo-two-dimensional, P2D, model, (with one-dimensional heat generation), consisting of a set of closely coupled nonlinear partial differential equations. These equations are reformed to a set of ordinary differential equations which can be solved using the MATLAB function 'IDA' (43).

Torchio et al. (43), validate LIONSIMBA by comparing the predictions from a standard 1C charge and discharge with the predictions made by COMSOL MultiPhysics and DUALFOIL. Near identical cell potentials, electrolyte concentrations, temperatures and surface solid-phase concentrations were obtained, with significantly faster simulation times. They propose that this is due to the underlying numerical algorithm used by LIONSIMBA, which is more efficient than in the other models. This validation, combined with its incorporation of heat generation, mean the following predictions generated by LIONSIMBA are a reliable starting point for this project.

Modelling predictions used predominantly as a base line to compare and narrow down on specific strategy types, which will later be experimented with. Only comparative results between different strategies were therefore required, and highly accurate quantitative data was not necessary. ΔT was selected as a method for determining the success of the profile due to it links with cell degradation and lifetime (44).

An offline copy of the model was created from the 'GitHub' repository. All edits currently remain local and have not yet been shared with other developers. As will be mentioned in section 7, it is hoped that the newly developed code that will be discussed shortly will be uploaded to GitHub to add a CT charging capability to the model.

Initially, the model was parametrised with data based on a 60Ah pouch cell. These data were already imbedded within the model and members of the Imperial College London battery group, (for example, Weilong Ai), suggested that the results would be similar enough to those parametrised for 21700s, to be used in a comparative way (13). By editing the embedded 'Initial Parameters' script, it was ensured that the model would run with natural convection, to mimic both the experiments to come and an EV battery pack with simple cooling.

The unchanged model allowed CC-CV to be run at a selected C-rate. Time was spent to program pulse, negative pulse and MCC-CV charging, specifically ensuring that the charge time matched the C-rate inputted by the user and that the ΔT could therefore be compared across profiles. The functions which were written to achieve this were collated in a 'Master Script'. This new script can be run, and an interactive user interface now allows the user to select the specifics of the profile they wish to model with.

3.2 Modelling Results and Adaptations

Both pulse and negative pulse charging remain a controversial topic of research, with many conflicting results from both models and experiments (45). A wide variety of pulse profiles were tested using the model, however none appeared to reduce ΔT of the cell when compared to a CC-CV profile of identical charge time. Figure 8, shows results for one of these profiles. It is worth reiterating, however, that ΔT is not a direct indication of degradation and capacity fade, merely a factor of it. It cannot, therefore, be concluded that there is no benefit from pulse charging from these preliminary results.

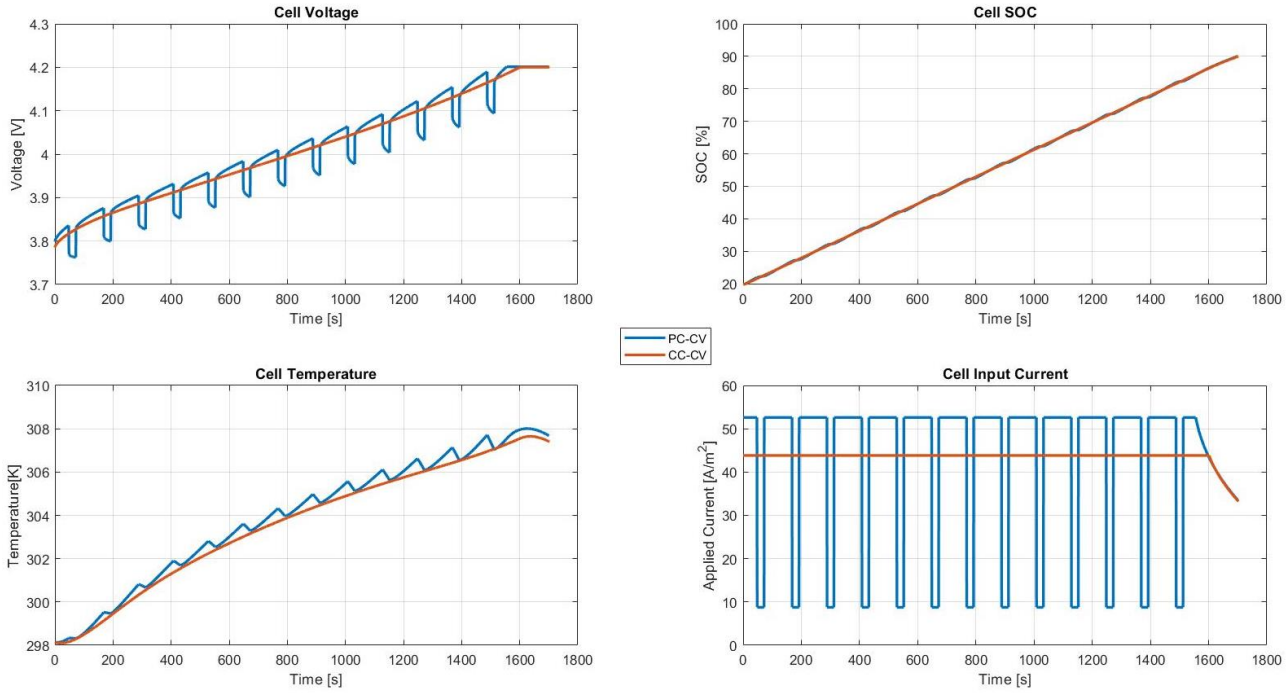

Figure 8 - LIONSIMBA results for a PC-CV profile

Multistage profiles are less controversial, however, and this is corroborated by the model. The majority of MCC and MCC-CV profiles tested produced a significantly lower ΔT when compared to CC-CV. The result for an MCC profile with five stages is shown in Figure 9.

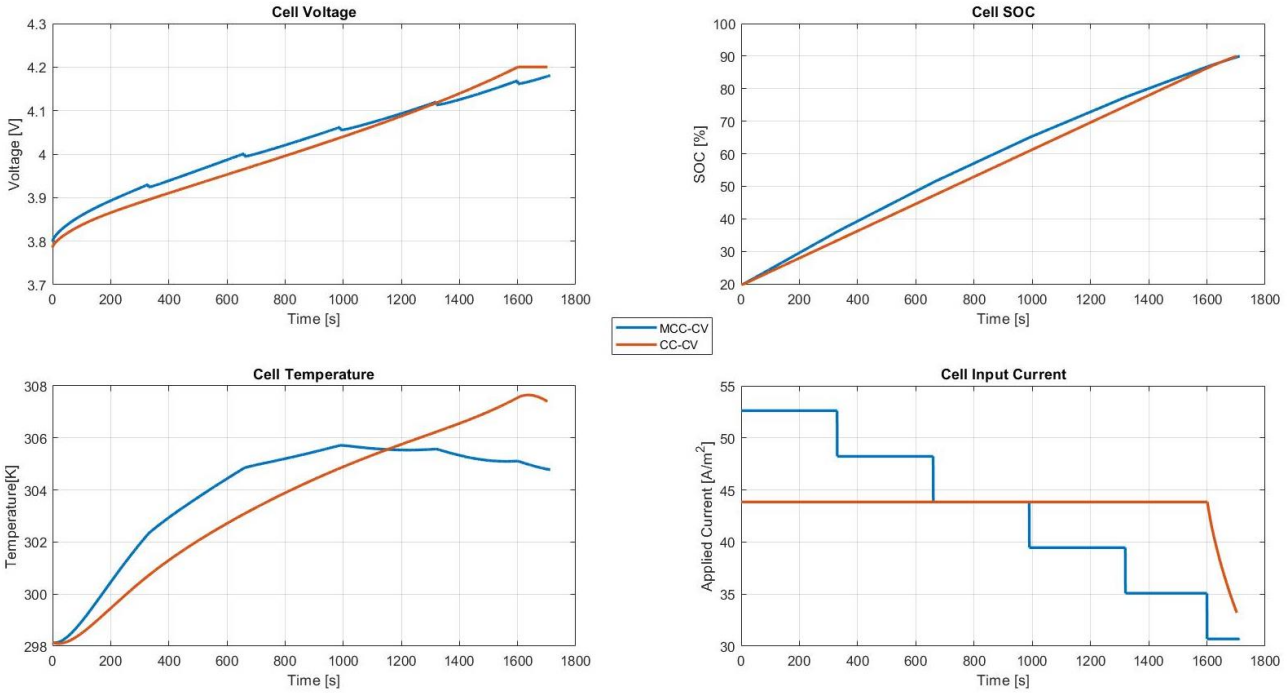

Figure 9 - LIONSIMBA results for an MCC profile

The high initial current, current profile shape and the plateau in ΔT caused by this MCC profile are indicative of CT charging strategies, and the successes of both are perhaps linked, rooted in their reduction in ΔT.

With CT charging strategies being the predominant focus of this project, the next step was to program these profiles into the model. LIONSIMBA can easily be parametrised to fix the cell's surface temperature, as if it is being maintained though strong convection or other cooling means. As previously emphasised, this is not the type of CT charging that is being investigated in this project. To the author's knowledge, LIONSIMBA has not be used in this way before, and a novel solution and code had to be created.

LIONSIMBA was not written with CT charging strategies in mind and, as such, the temperature parameter cannot be easily accessed whilst the simulation is running; it is embedded within over 50 functions, which are continuously updating the parameter. The surface temperature cannot therefore be used to adjust the current in real time, (as could be done experimentally using PID control and thermocouples).

To avoid this issue, an additional function was written which first executed the simulation with a CC-CV profile, and a subsequent profile was then created based off the temperature results of this previous run. This was repeated until the profile converged, and a CT profile was therefore formed. This additional function has also been integrated into the aforementioned 'Master Script'.

Whilst running a variety of CT strategies and continuing the literature review, it was realised that the significantly higher initial current seen in Patnaik et al.'s study may be damaging to the cell whilst not being entirely necessary. Figure 10 shows the results of a charging strategy which uses CC charging until the cell reaches a maximum temperature, before entering the CT stage.

It was found that strategies which utilised this method could reproduce the results of the leading paper in CT charging, (20% reduction in ΔT whilst maintaining the same charge time as a CC-CV profile (1)), without doubling, or even significantly increasing, the maximum current.

The term 'CC-CT-CV', (constant-current, constant-temperature, constant-voltage), was coined to describe these seemingly beneficial strategies.

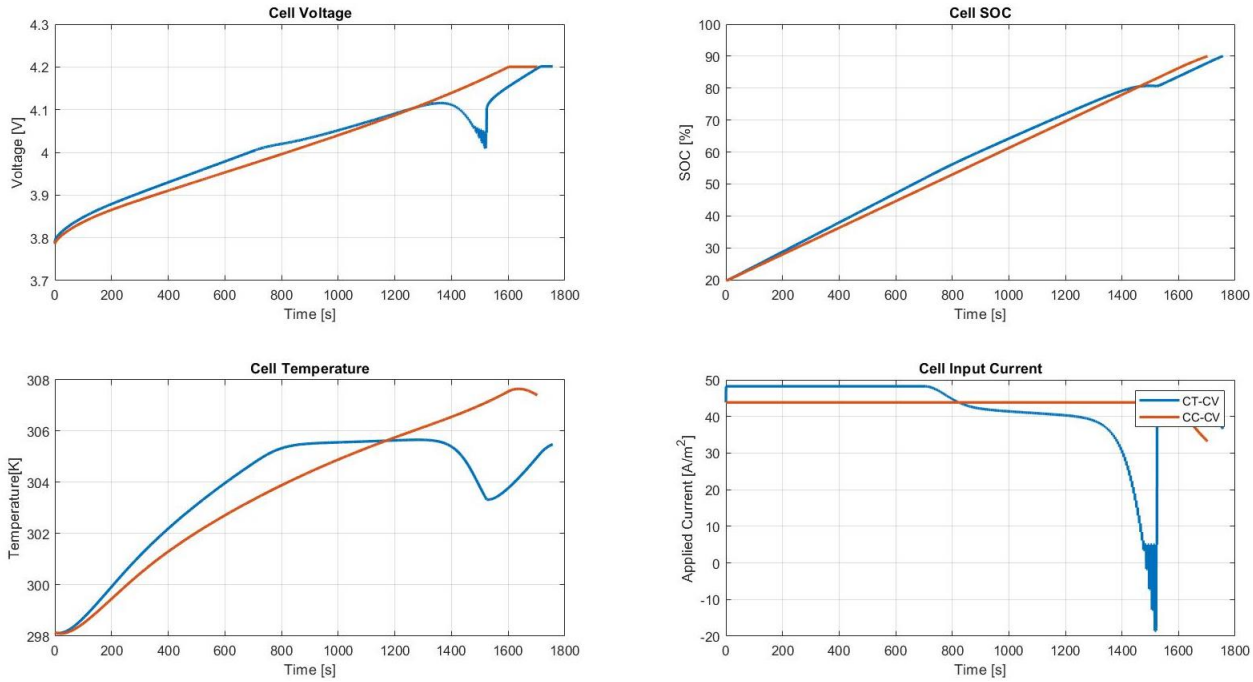

Figure 10 - LONSIMBA results for a CC-CT-CV profile

The simulation was formally run with 53 different current profiles, 24 of which were a type of CC-CT-CV. Each of these test lead to an improvement on the profile, culminating in the profile shown in

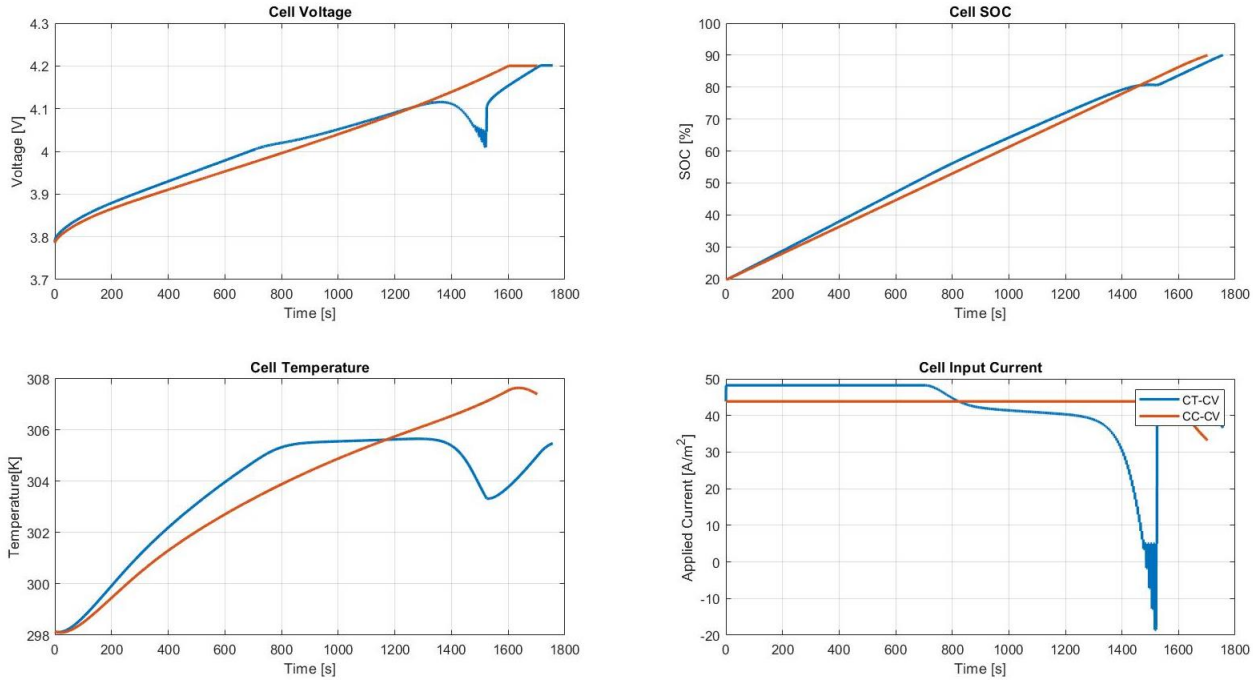

Figure *10*.

A **21.1%** decrease in ΔT, when compared to the CC-CV profile was achieved, with only minor increases in both the maximum current, I_{max}, 5.0%, and charge time, 3.2%. When compared to the 20% decrease in ΔT

for a 100% increase in I_{max} achieved by the CT-CV profile from Patnaik et al., the new CC-CT-CV strategy appears promising. This strategy would now undergo cyclic testing in a laboratory.

4. Procedures

4.1 Initial Plan

As aforementioned, when Patnaik et al. implemented their CT charging profile, they utilised PID control. Whenever an input needs to be adjusted to achieve and maintain a constant output, this technology is the go-to (46), and is therefore highly suited to this type of charging strategy. A previous student, Ben Hambrook, designed and built equipment which could be used to implement a range of current profiles, including those involving closed-loop feedback (8), (13). His design, however, relies on a piece of equipment called Kepco, an easily programable variable power supply unit, which remained out of use during this project. A new system, therefore, had to be developed. The cycling unit, called the Maccor, was used to achieve a quasi-CT profile, as explained in section 5.1. The procedures used during experimentation are outlined below. Where possible, a link to the official procedure has be provided, which contains detailed risk assessments and other additional information, however, all procedures are outlined in text.

4.2 Setup

Four LGM50s 21700s were initially setup for experimentation. All setup and experiments occurred in laboratory 101. Whilst not in use, the cells were kept in an insulated box in refrigerators. All exposed electrical contacts were coved in the insulating tape, Kapton, unless the area needed to be accessed.

First, nickel tabs were spot welded onto both ends of the cell using the Sunkko 709AD+ spot welder in accordance with the following procedure:

https://wiki.imperial.ac.uk/pages/viewpage.action?pageId=120893020

Both the tabs and the cell were cleaned with isopropanol to reduce electrical resistance. Figure 11 shows the positioning of the nickel strips on the cell, as well as the position of the two welds on each tab.

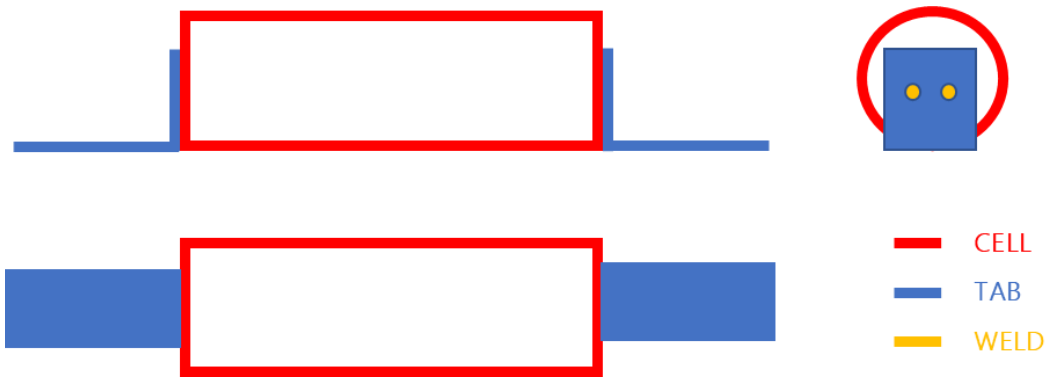

Figure 11 - Positioning of the nickel tabs

Rigs to house the cells were modified from existing 18650s rigs. In order to fit the slightly larger 21700s, additional holes were drilled into the acrylic base to move the brass contact blocks further apart. Figure 12 shows a labelled image of the rigs and demonstrates the size adjustment.

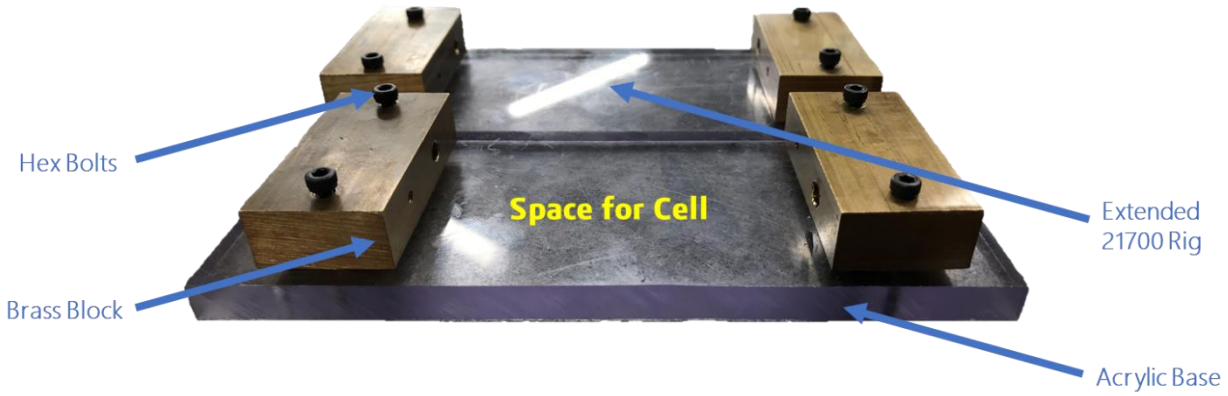

Figure 12 - Labelled image of rigs

In order to attach a cell to a rig, the bolts were loosened, and the nickel tabs were 'sandwiched' between the brass blocks and the acrylic. The base of the blocks and the tabs were polished and cleaned with isopropanol prior to this. The screws were then tightened to minimise the contact resistance.

The contact resistances were measured using a high accuracy voltage meter across the blocks. This was repeated three times and the average results are provided in Table 2.

Table 2 - Contact resistance results

Average Contact Resistance	Cell C / CC-CV	Cell D / CC-CT-CV
Negative Electrode / mΩ	0.57	1.17
Positive Electrode / mΩ	0.62	0.45

It is worth noting that cells A and B were set up and spot welded but never used. The contact resistance at cell D's negative electrode is roughly double that measured at the other electrodes. This could have been caused by a slightly rougher surface on the brass block or on the tab, or a poor spot weld. The implications of this are discussed in section 6.2.

The rigs were placed inside separate thermal chambers, which were maintained at 25°C, to mimic natural convection conditions. The cells were connected to the Maccor via wires at each electrode, (holes were drilled into the brass blocks to create contacts for these wires). Thermocouples were attached to the cell using thermally conductive epoxy, one at the centre and one at each end, with an additional T-type

thermocouple in the centre, (the T-type can be connected to the Maccor and provide the necessary feedback to create a CT strategy). This layout is shown in Figure 13.

Figure 13 - Thermocouple layout

All thermocouples, apart from the T-type, were connected to a Pico-Logger, which in tun was connected to a laptop to record the temperatures. A thermocouple was also setup away from the cell inside the chamber to ensure 25°C was maintained. The final setup of the cells can be seen in Figure 14, where they remained for all further experiments.

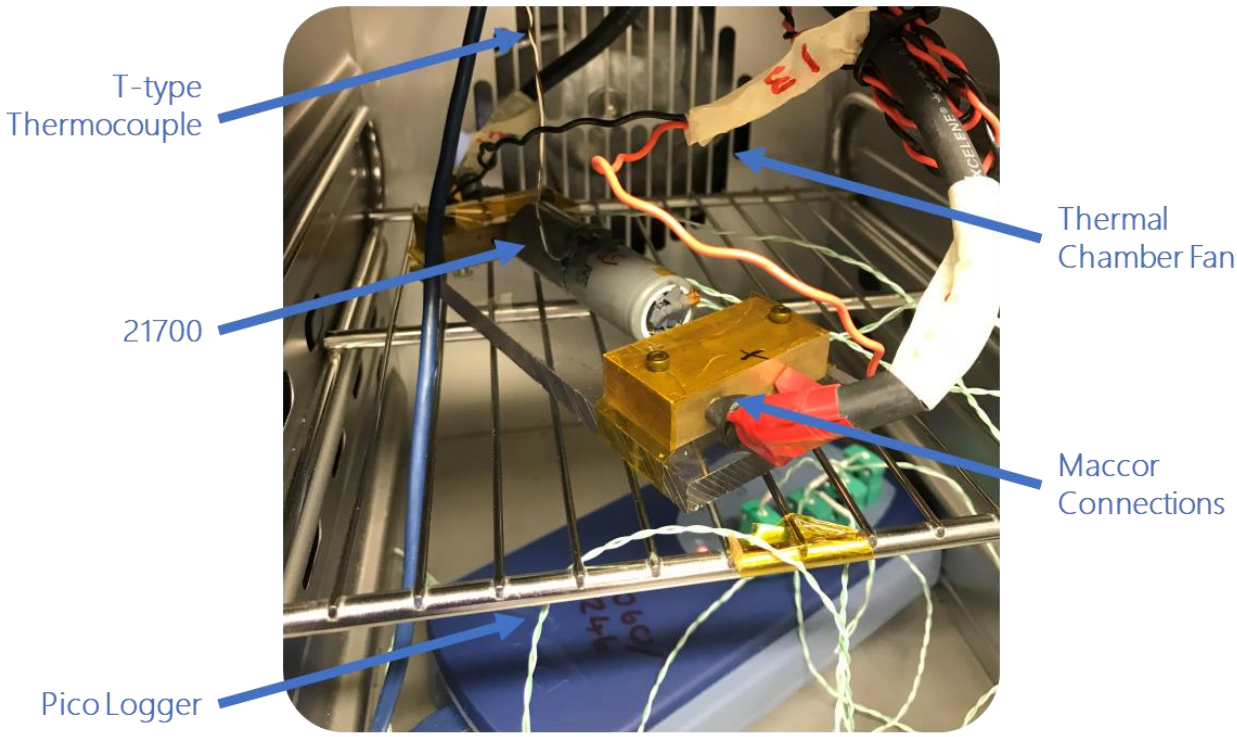

Figure 14 - Final set up of cell

4.3 Initial Characterisation

An OCV test and pulse test were performed at beginning of life, BOL, to obtain the initial capacities and resistances. The OCV test begins with a long rest, (ensuring the thermal chamber reaches steady-state conditions), a 0.3C charge and another long rest. This ensured the cell is fully charge. A C/24 discharge followed by a C/24 charge completes the test.

Pulses were performed at six C-rates, (C/20, C/10, C/4, C/2, 1C, 1.5C), for 10 seconds followed by a 100 second rest. Pulse testing begin at 100% and the pulses occurred at four SOCs, (80%, 60%, 40%, 20%). The sampling frequency of the Maccor was increased, from 1 Hz to 100 Hz, during pulse testing to ensure the voltage response of the cell was sufficiently captured.

The procedure for the pulse test is provided below:

https://wiki.imperial.ac.uk/display/EESE/Test+Plan+-+LG+M50+Parameterisation%2C+Pulse+Testing+-+Jake+Reynolds+-+FYP

4.4 Cycling

After the CT profile was developed using the Maccor's software, see section 5.1, cycling could begin. Each cell was charge with either the 0.7C CC-CV control or the CC-CT-CV profile detailed in section 5. Both cells were discharged with an identical CC, at 0.7C. Characterisation, in the form of an OCV test and pulse test, would occur every 50 cycles. The characterisations which took place during cycling were identical to the ones conducted at BOL described above.

Links to the specific test procedures, (for CC-CT-CV and CC-CV cycling respectfully), are provided below:

https://wiki.imperial.ac.uk/display/EESE/Test+Plan+-+LG+M50+Constant+Temperature+-+Cycling+-+Jake+Reynolds+-+FYP

https://wiki.imperial.ac.uk/display/EESE/Test+Plan+-+LG+M50+CC+-+Cycling+-+Jake+Reynolds+-+FYP

4.5 Adjustments

Initially, cycling was due to continue until both cells reached 300 cycles. Due to delays and disruption caused by COVID-19, see section 6.1, only 200 cycles were reached. Further, the memory capacity of the Maccor was reached on numerous occasions, meaning that characterisation occurred at slightly misaligned points.

It is worth nothing that the first 30 cycles or so on both cells were done using a CC-CV profile, as the pre-set temperature to begin the CT stage was never reached, and the code controlling the CT strategy had to be updated remotely.

Data processing includes, but is not limited to, plotting raw data, Coulomb counting, fitting an ECN model to the pulse data and applying filtering techniques to obtain the IC plots.

5. Experimental Results

The key results of these experiments are presented here in three distinct sections. First, the ability to achieve CT charging without PID control is shown. Second, the general performance results, revolving around charge time and ΔT, of both the CC-CV and CC-CT-CV profiles are provided. Finally, and perhaps most significantly, the results of the degradation studies are presented.

5.1 Producing CT Charging

As alluded to above, one aspect of the experiments was to determine if CT charging could be achieved using the relatively crude coding found in the Maccor's software. This process was iterative, given that, as far as could be identified, the Maccor and its software had never been used in this way before. An expert from Maccor, David Smith, was contacted and he gave initial advice on the functions which can be implemented within the software.

Using the 'IF' formulas present within the software, a 'Bang-Bang' approach to CT charging was achieved. Essentially, if the surface temperature of the cell exceeded a present value, the current would linearly and gradually reduce until the temperature fell below this value. The current would then immediately return to the original current, identical to that used in the initial CC stage of charging.

The 'Bang-Bang' approach is also used by the heat chambers which kept the ambient temperature of the cells' constant through cycling. It is these chambers that provided the inspiration for achieving CT charging without PID control.

The initial current, the rate at which the current decreases, and the pre-set temperature were based on the predictions from modelling and were fine-tuned through trial and error. It is worth noting that this means that the CT cell underwent some short charging periods, however these are accounted for in the results. Examples of runs during this trial and error process are provided in Figure 15, where changes in time scales should be noted.

The top current profile shows an attempt where the current remains at its maximum if the temperature is above the pre-set value, and at zero if it is below. The middle image shows the first time the current decreased gradually, however this decrease is much more rapid than what was achieved computationally and would most likely result in a large overcorrection in temperature. The bottom image shows an improvement to this, whereby the current reduces over a three-minute period and does not reach zero before the temperature reduces to the required level.

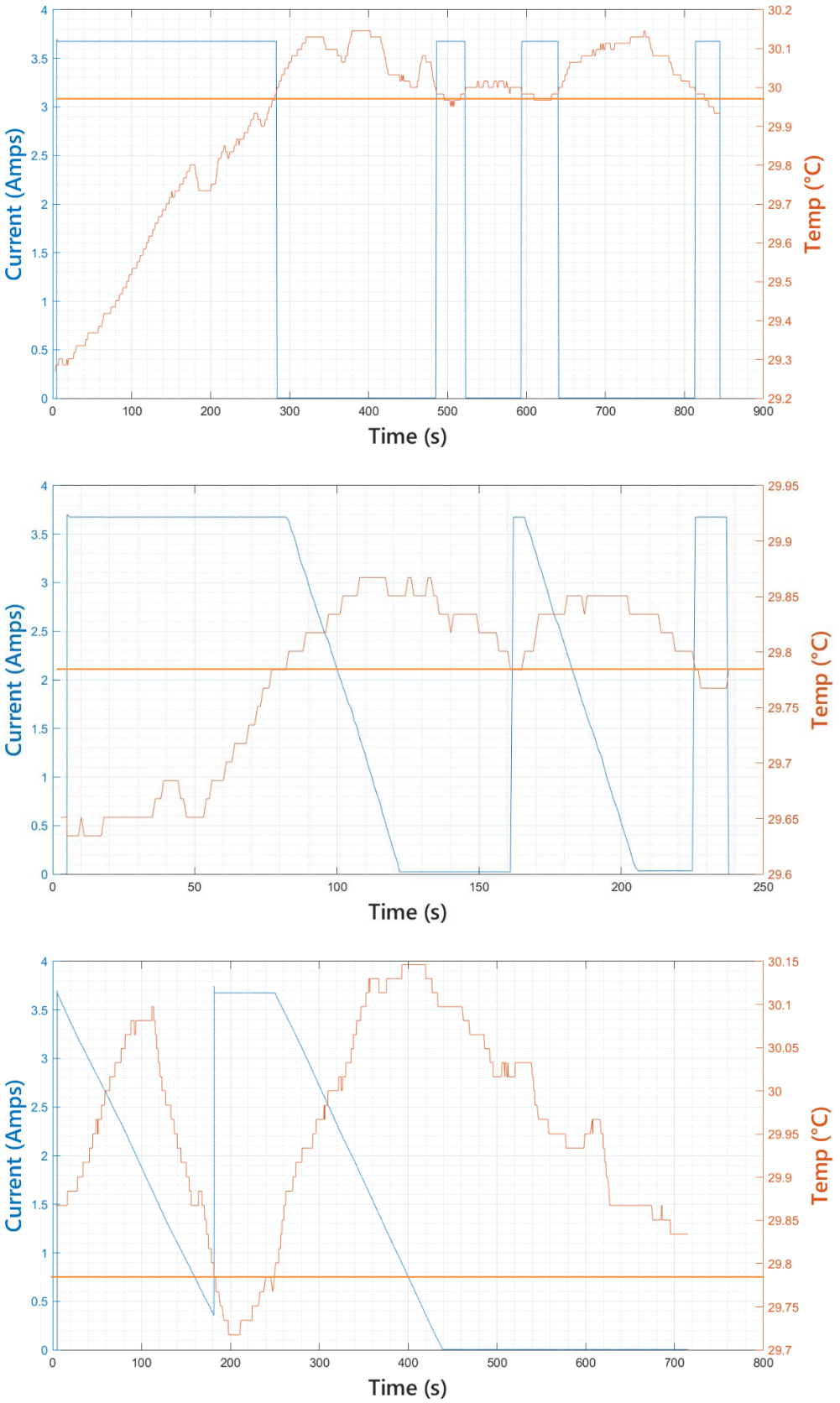

Figure 15 - Top) an initial attempt where current is binary; on or off, Middle) current decreases linearly, however the decrease is rapid and reaches zero within 50 seconds, Bottom) decease is more gradual

Figure 16 shows a complete charge using the novel CC-CT-CV developed. There is a clear initial temperature rise during the CC stage, followed by the CT stage which is automatically triggered when the temperature rises to a pre-set value of 27.1°C. Due to the 'Bang-Bang' approached used, the temperate fluctuates around this level, by around ±0.5°C. As with the results shown during modelling, these fluctuations would be removed almost completely with the incorporation of PID control.

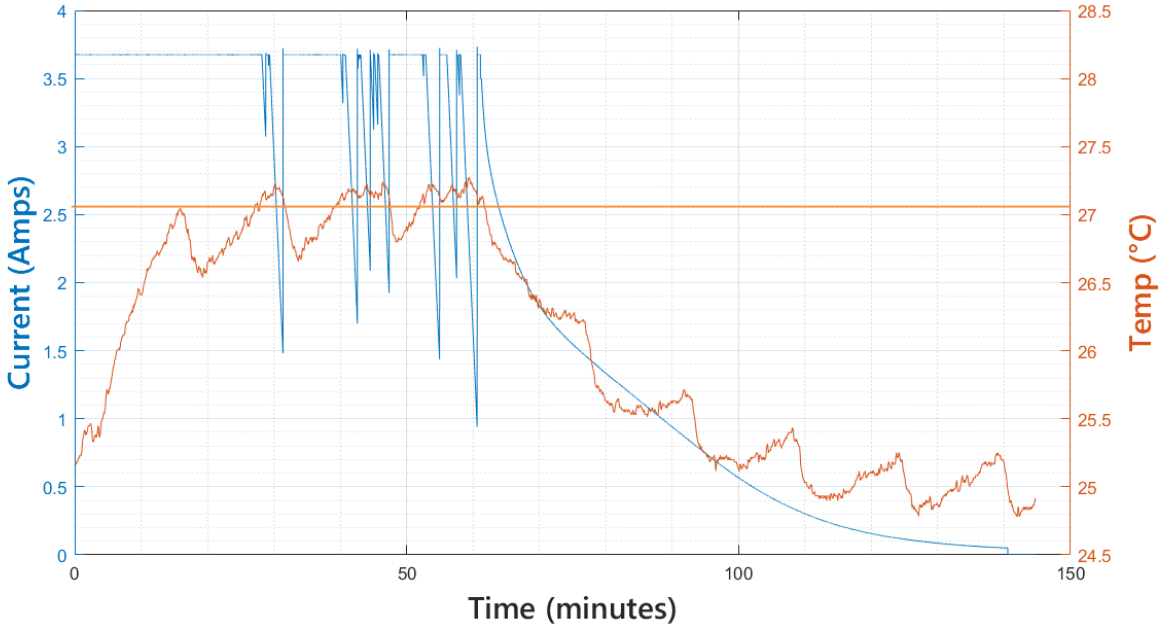

Figure 16 - Final CC-CT-CV profile used

For comparison, Figure 17 shows the CC-CV profile which is cycled on a separate cell as a control.

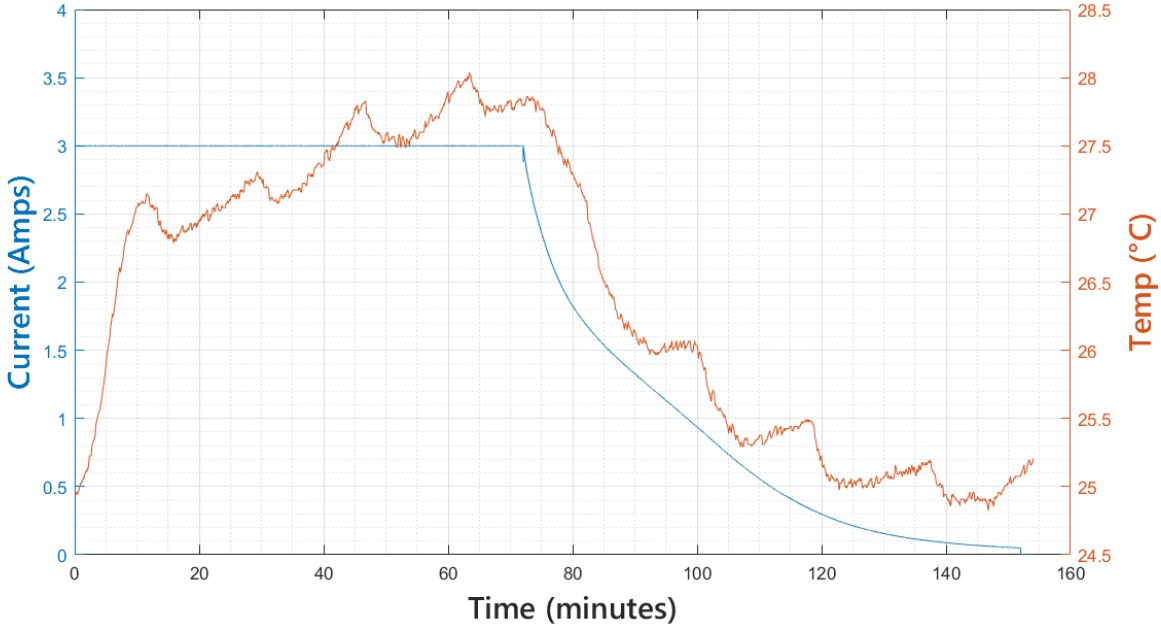

Figure 17 - CC-CV profile used as a control

5.2 Performance Results

As will be discussed in detail in section 6, the CC-CT-CV profile developed here outperformed Patnaik et al.'s CT strategy, as well as the CC-CV profile that was used as a control. Table 3 provides the numerical differences of both profiles when compared to their respective control CC-CV profiles.

Table 3 - Comparison of the improvements achieved by the novel CC-CT-CV and the existing CT-CV profile when compared to their respective controls

	Novel CC-CT-CV Profile	Existing CT-CV Profile
% Change in Charge time	**-7.4%**	0%
% Change in ΔT	**-28.7%**	-20.2% *
% Change in I_{max}	**+23.2%**	+100%

* the 20.2% reduction in ΔT could be applied to the charge time instead in an either/or situation. For the novel profile, a reduction in both can be achieved simultaneously.

The most preferential result is presented in bold. By providing a reduction in charge time, whilst simultaneously reducing the temperature increase, and with only a slight increase in the maximum current, the novel strategy clearly outperforms the existing one. Figure 18 shows a complete cycle of both CC-CV and CC-CT-CV charging, making these improvements clear.

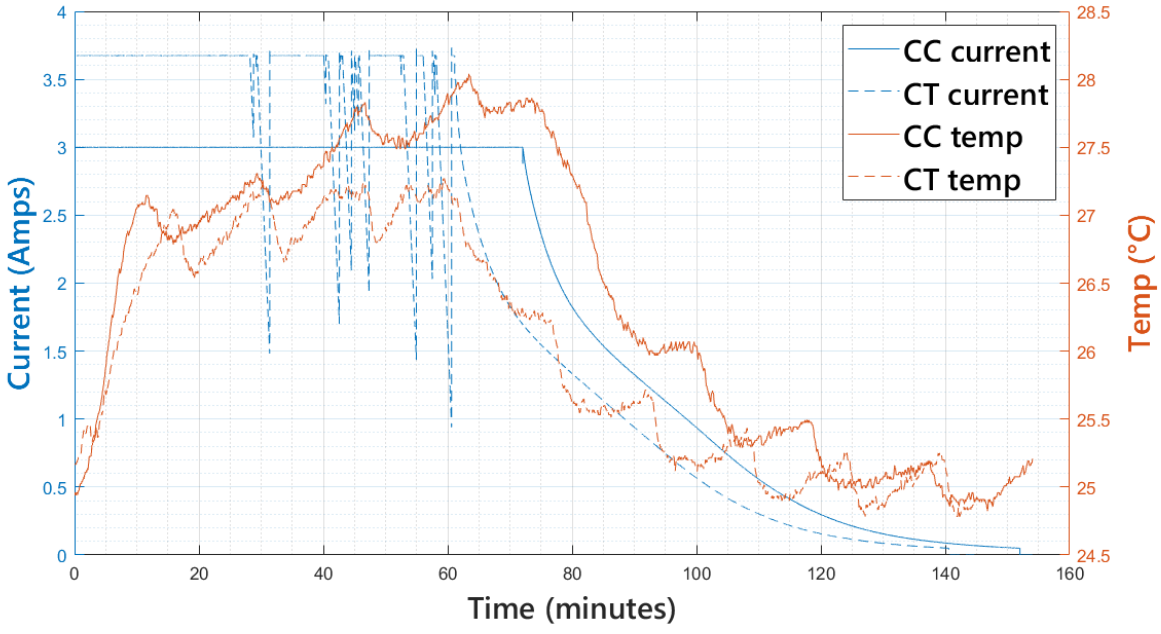

Figure 18 – A full cycle for both CC-CV and CC-CC-CV

5.2 OCV

As discussed in the literature review, an OCV test was performed regularly to obtain the capacity of the cell, and thus, the capacity fade caused due to cycling. Figure 19 and Figure 20 show a C/24 charge and discharge of the cells used for CC-CV and CC-CT-CV charging respectively. This OCV test was performed at BOL.

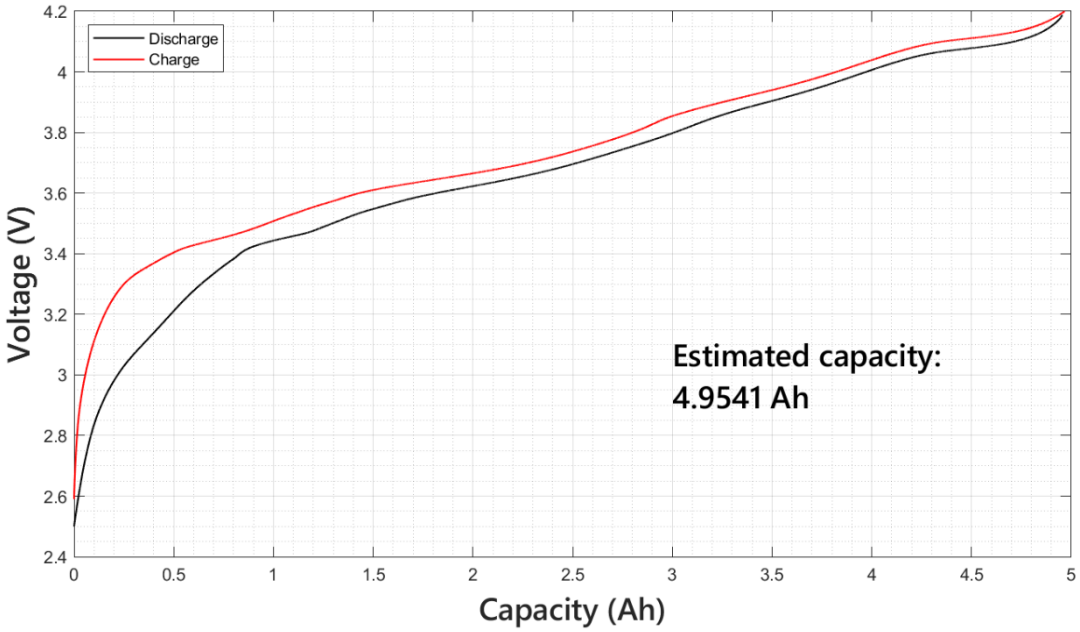

Figure 19 - BOL OCV test for the cell to be cycled with CC-CV

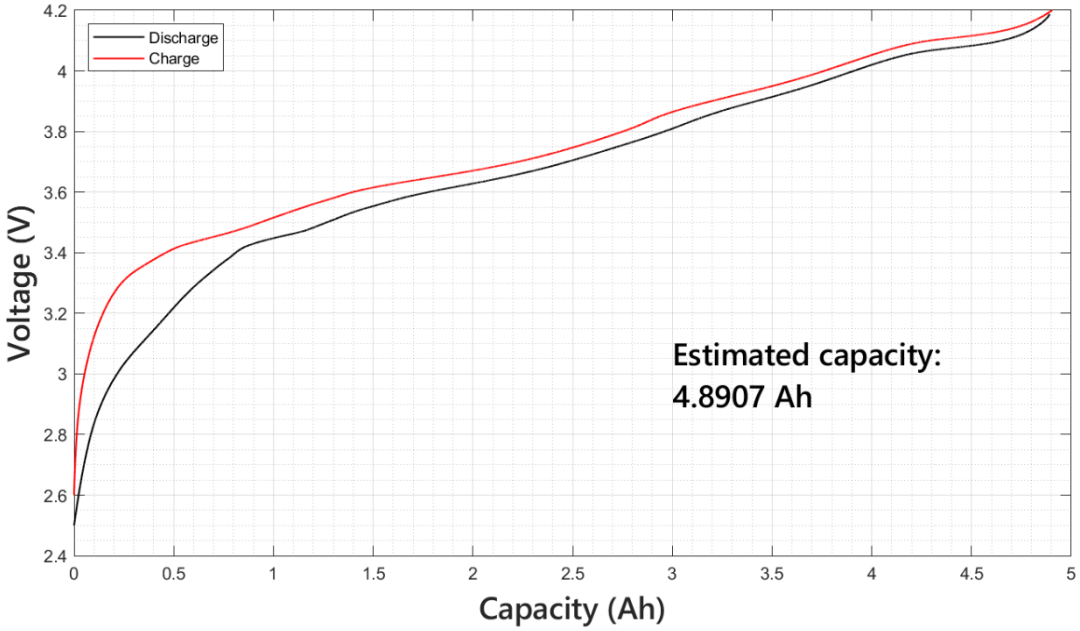

Figure 20 - BOL OCV test for the cell to be cycled with CC-CT-CV

The capacity of the cell is calculated from the data obtained in this experiment using the method outlined in section 2. As can be seen in Figure 19 and Figure 20, the BOL capacity can vary greatly from the manufacturer's rated value, (5 Ah in this case, >2% deviation), and this initial test is crucial so that any capacity fade which occurs can be compared fairly. To compare the results with ease, the capacity of each cell, (in terms of a percentage of the original capacity), is plotted against the number of cycles since BOL in Figure 21.

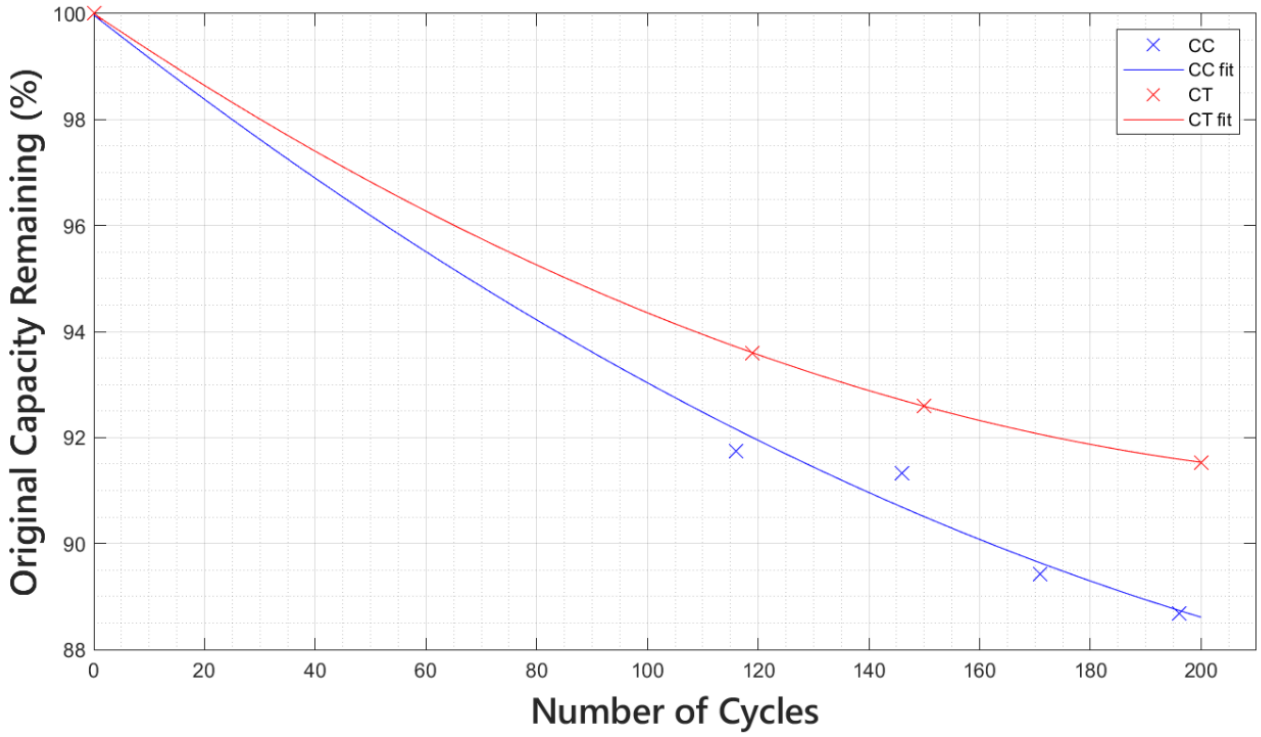

Figure 21 - Percentage of original capacity remaining vs number of cycles since BOL for both CC-CV and CC-CT-CV cycling

Perhaps the most substantial results to notice here is that from BOL until the 200th cycle (or 196th for CC-CV, both are the maximum number of cycles achieved during these experiments), the capacity fade is greater for the original CC-CV profile. Table 4 provides capacity fade, as a percentage of original capacity, after the final cycle is complete for both charging strategies.

Table 4 - Capacity fade caused by CC-CT-CV and CC-CV after the 200th and 196th cycle respectively

	Capacity Fade / %
CC-CV	11.3%
CC-CT-CV	8.5%

In other words, this CT strategy reduces capacity fade by **24.8%** when compared to CC-CV.

5.3 ICA

IC plots are provided for both CC-CV and CC-CT-CV cycling in Figure 22 and Figure 23 respectively.

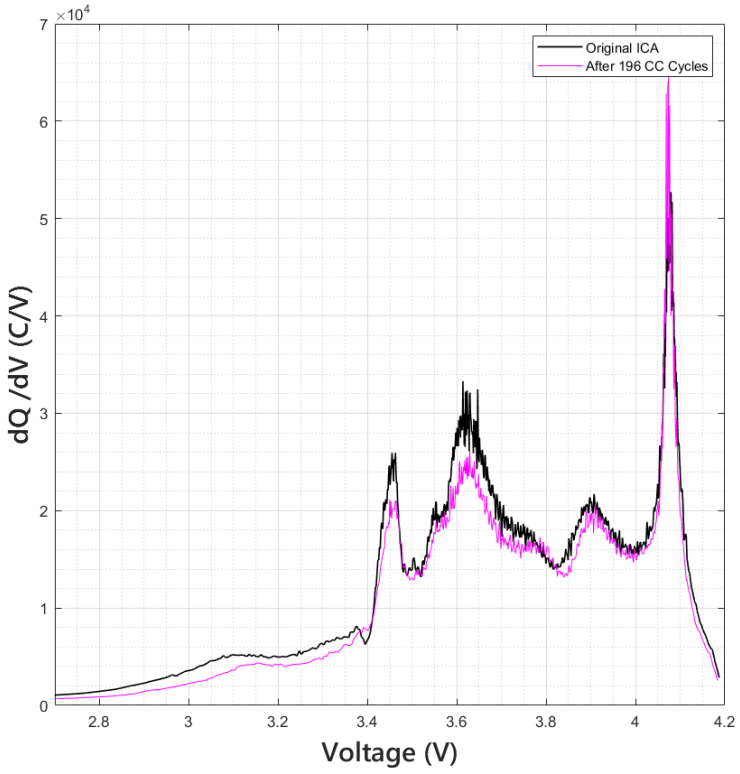

Figure 22 - ICA at BOL and at the end of cycling for the cell cycled using CC-CV

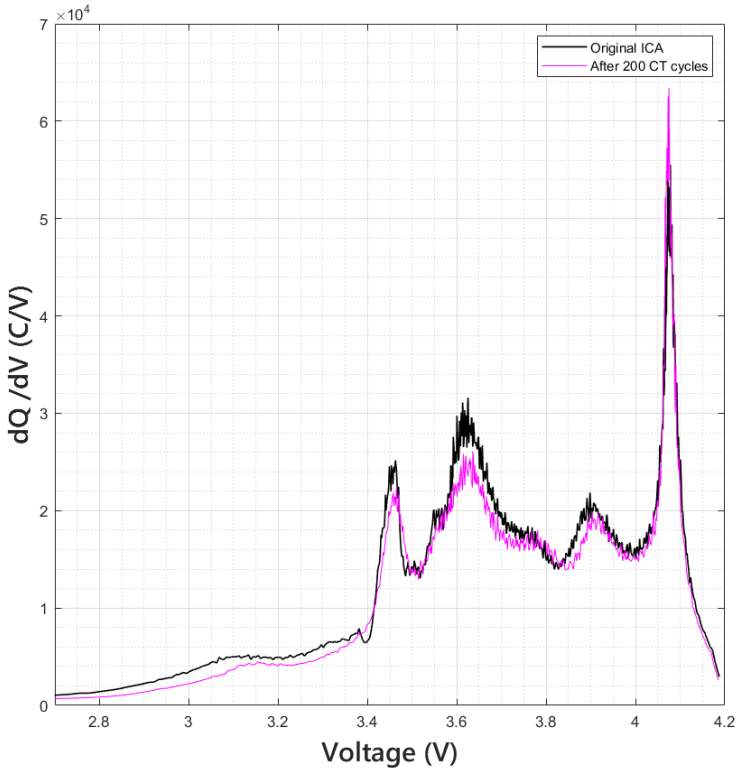

Figure 23 - ICA at BOL and at the end of cycling for the cell cycled using CC-CT-CV

As will be discussed, the position and movement of peaks provides insight into the degradation mechanisms which are occurring within the cell. Figure 24 zooms into sections of the IC plots. The slight movements which can be seen here will be compared and discussed, albeit briefly, in section 6.

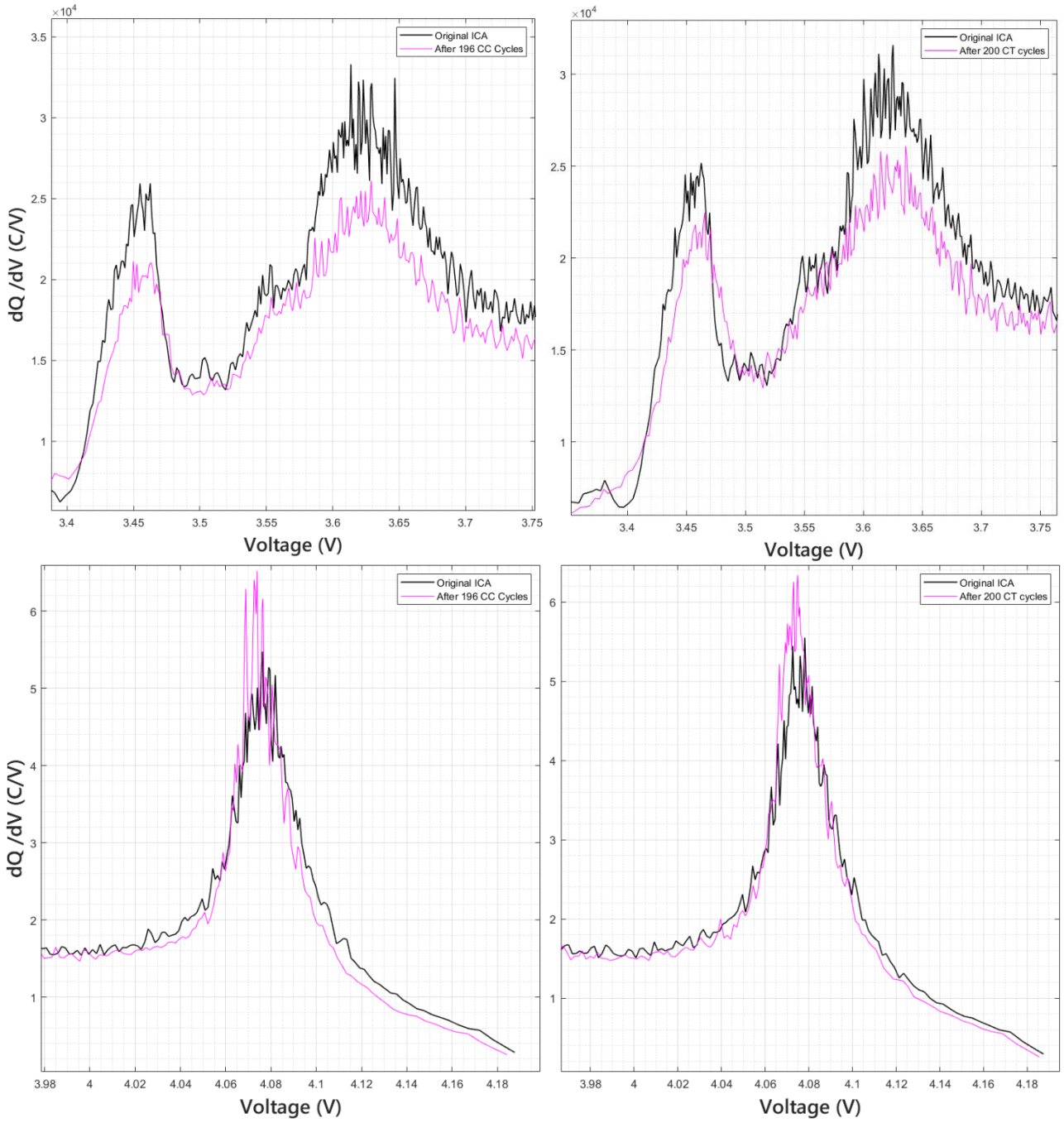

Figure 24 - Zoomed versions of the IC plots. Top Left) First two peaks for CC-CV cycling, Top Right) First two peaks for CC-CT-CV cycling, Bottom Left) Last peak for CC-CV cycling, Bottom Right) Last peak for CC-CT-CV cycling

5.4 Pulse

An example of the raw data collected from pulse testing is provided in Figure 25. These data were collected during a BOL pulse test on cell D, which was used for cycling the CC-CT-CV profile.

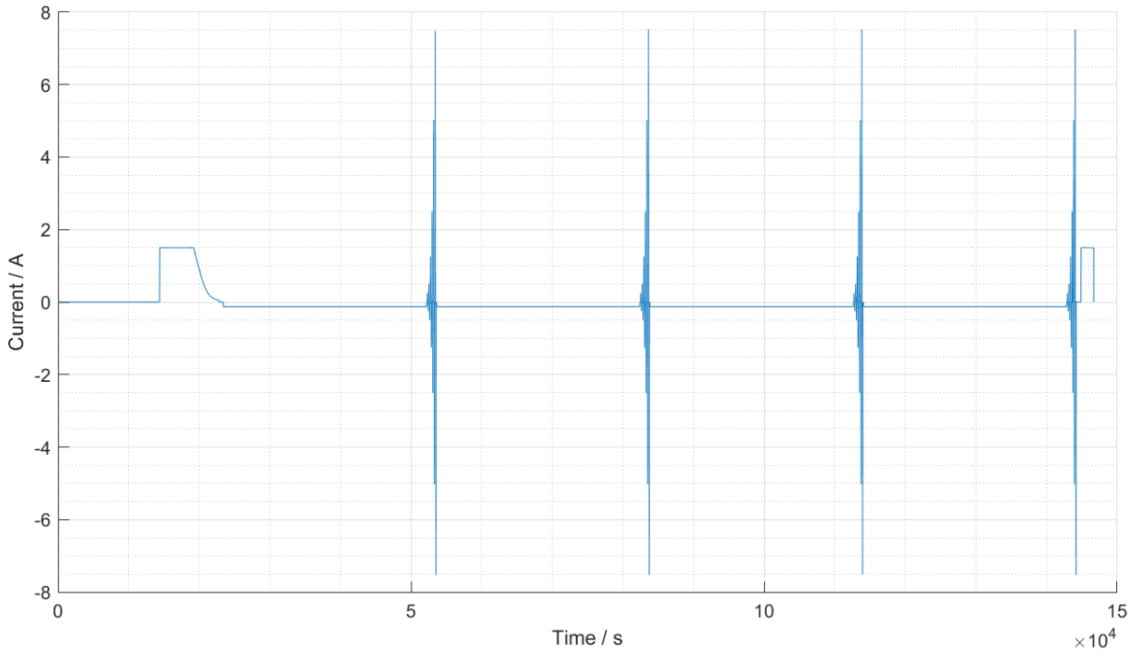

Figure 25 - Raw current/time data from a pulse test

Figure 26 shows the voltage/time response measured during pulsing. The resemblance to Figure 4, (a labelled voltage response from a pulse provided in the literature review section), is evident.

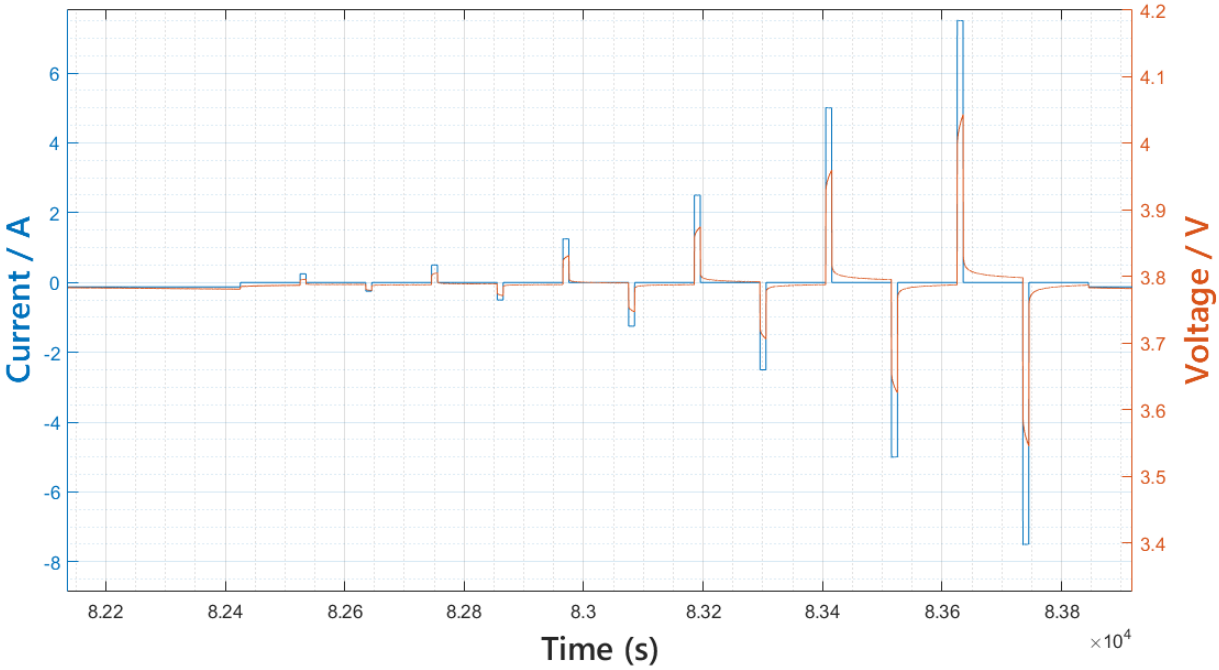

Figure 26 - Raw current/time and voltage/time data from a pulse test at a particular SOC (80%)

As aforementioned, this voltage response is then fitted to the ECN model to obtain values for the ohmic resistance, R0, at difference SOCs and C-rates. An example of the data obtained is shown in Figure 27.

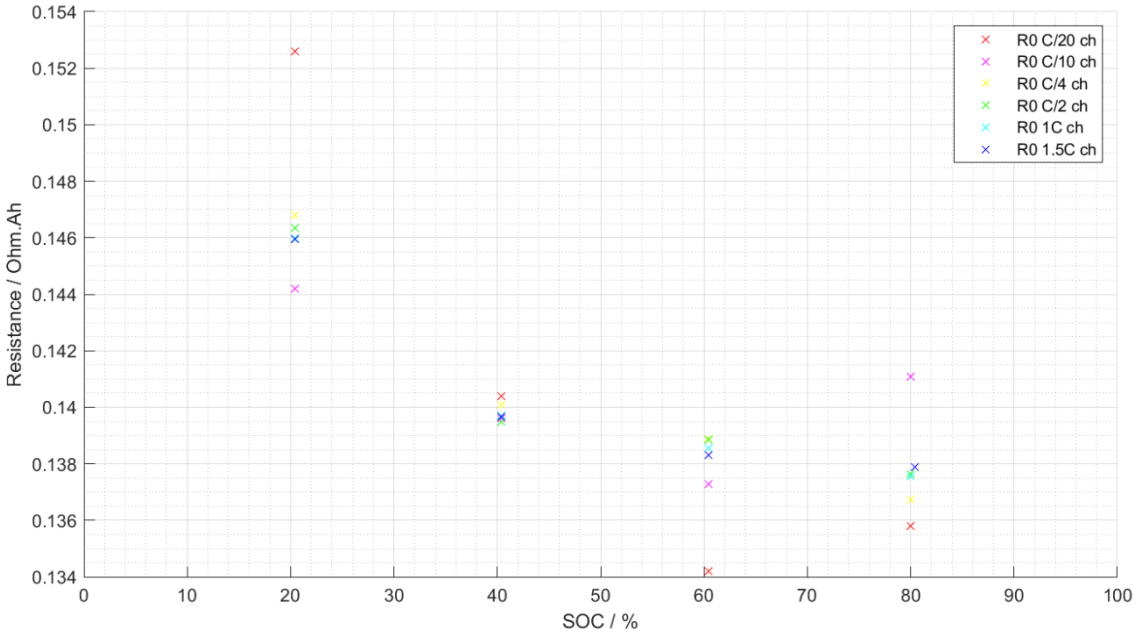

Figure 27 - Normalised ohmic resistance vs SOC at BOL for cell D

It is important to note that Figure 27 is merely an example of the results. For each cell, both the lumped and ohmic resistance are obtained at each C-rate. This occurred at each of the characterisation points for both CC-CV (five times), and CC-CT-CV, (four times). These types of plots are useful to compare trends in how the resistance varies depending on SOC and C-rate. These trends are not of interest here. Instead, the change in ohmic and lumped resistances are compared in Figure 28 and Figure 29 respectively.

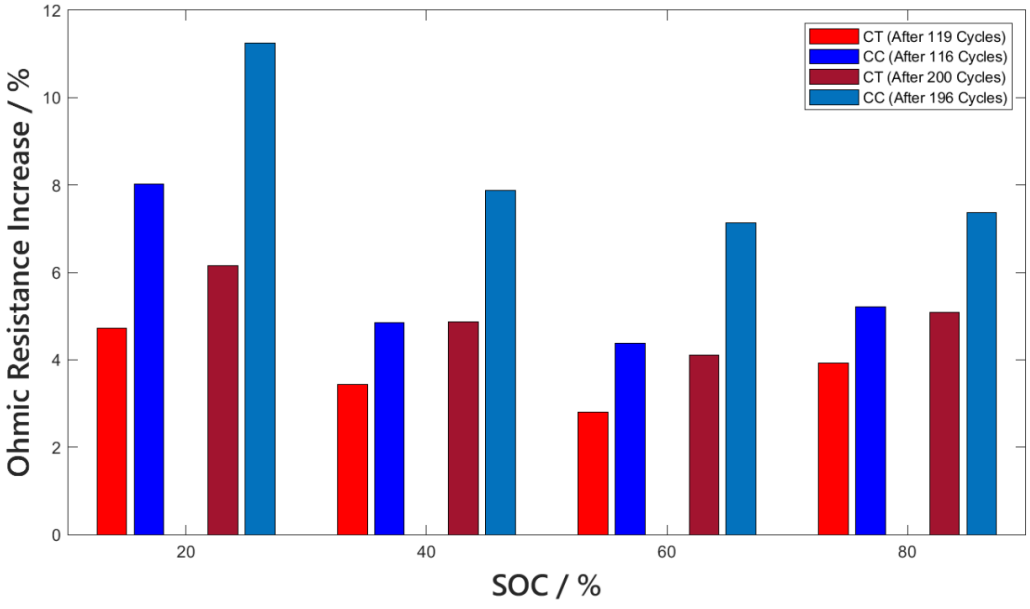

Figure 28 - Ohmic resistance increases at C/2 charging

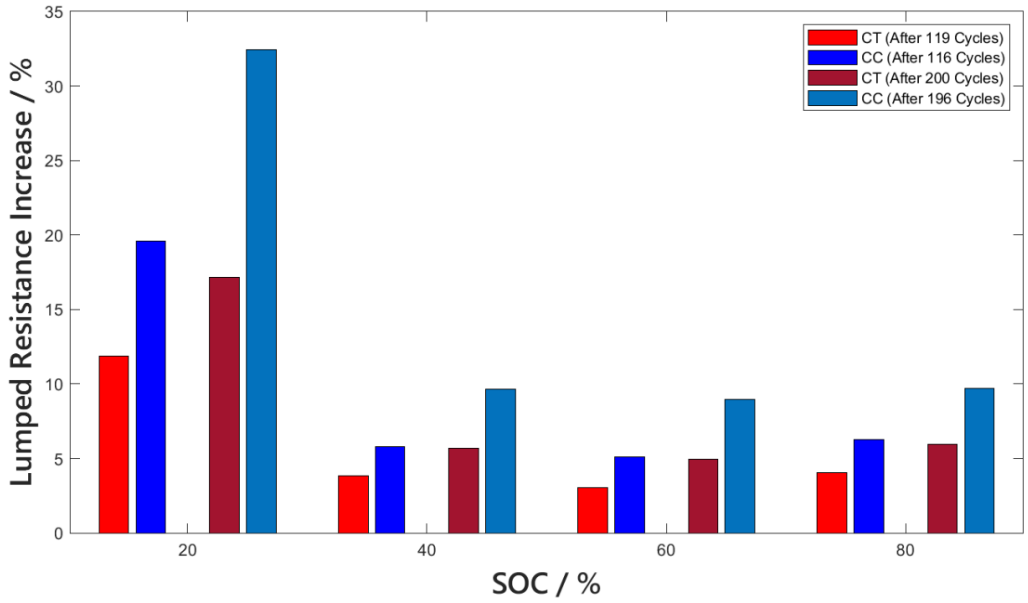

Figure 29 - Lumped resistance increases at C/2 charging

Once again, these results are taken at a particular C-rate, C/2, as, as expected, there is little to no variation in the percentage change in resistance across the C-rates, (pulsing at different currents will not affect the amount of degradation that has already occurred, nor will it record a different amount).

After cycling, the CT strategy results in a **45% reduction** in R_0 increase when compared with the CC-CV strategy, and a similar **47% reduction** in lumped resistance increase.

-

It is worth noting that the true value of pulse testing *does* come when comparing the trends in resistance in a singular cell, rather obtaining exact resistances to compare across cells. For more precise values, a Galvanostatic Intermittent Titration Technique, GITT, test could be used to parametrise the ECN model at multiple temperatures. Nevertheless, the percentage increases shown here do show that the internal resistance of the cell cycled with CC-CV increase significantly more than the cell cycled with CC-CT-CV.

6 Discussion

6.1 COVID-19

On March 26th, 2020, laboratory 101 was closed to personnel, except for a handful of volunteers. These volunteers monitored and updated ongoing projects deemed to be 'essential to the group's research' and 'within probable sight of publication'. This project was considered to fulfil these criteria and permission was granted for these experiments to continue.

As expected, some disruption did occur. This includes a lack of response from the Maccor Expert, David Smith, from March 4th onwards, and a reduction in the amount of time spent fine-tuning the CT profile to be used in cycling. The cells used for these 'fine-tuning tests' also had to be used for cycling, as there was no time reset the rigs. The BOL characterisation occurred before these tests, which have been accounted for in the number of cycles; this explains the slight misalignment in when the characterisation tests occurred for each cell.

Some issues were also encountered when editing existing Maccor scripts, resulting in no characterisation test occurring for the CT strategy at around 170 cycles. None of these issues, however, prevented data from being obtained, thanks to the ESE Group at Imperial College London and the individuals who edited, monitored and exported data from these experiments.

6.2 Caution

Before discussing the effects of the novel CT charging strategy, it is worth addressing any potential issues with both the methodology and results.

First, both the CT strategy itself and the specific charging profile are considered. The profile was developed in part using trial and error, and, due to time constraints, the first profile which produced a relatively constant temperature was used for cycling. Whilst unlikely, it is possible that, coincidently, this profile is extremely optimised, and is one of the only CC-CT-CV profiles to produce the significant results shown here. Only conclusions regarding this specific profile can therefore be made; caution should be exercised when referring to the CC-CT-CV strategy in general. Future work on a variety of profiles should be performed, including those which adopt PID control, thereby reducing the temperature fluctuations.

Further, it should be noted that the temperature referred to in CT charging is recorded by the thermocouples which are attached to the cell at its *surface* and in the *centre*. An underlying assumption is that by keeping this temperature constant, the internal temperature, where degradation occurs, will remain

more constant. This temperature, however, has not been measured directly and this should be acknowledged when explaining why CT charging has certain effects on the cell.

Second, the methods used to collect these data are considered. The contact resistances of the cells in their rigs were determined, and a resistance of 1.17 mΩ was recorded at the negative electrode of cell D. Whilst it is still significantly less than the ohmic resistances found during pulse testing (still >5%, although this could be due to an overestimation for R_0), it is double the other contact resistances. Two strategies were used to amend this. First, cell D was used to test the CC-CT-CV profile, such that any promising results could not be discredited by a lower contact resistance, and second, all final results are provided in terms of a percentage change from the initial BOL value. The latter will also help when comparing these results with any future experiments.

Due to initial testing and the disruption explained above, the characterisation tests are slightly misaligned. Results, however, are only compared where the CC-CT-CV strategy has been cycled more than the CC-CV; for example, 200 cycles of CC-CT-CV vs 196 cycles of CC-CV. This would mean that the cell cycling the CT strategy would have degraded further than the other cell if the strategies performed the same and removes any doubt that could be cast on the results. Finally, it should be noted that as cycling continues, the capacity fades whilst the charging current remains constant. This means that the effective C-rate increases. After any number of cycles, the cell degrading faster will be charging, and discharging, at a higher C-rate. There is currently no simple fix for this issue, however, many papers ignore this, and it is worth considering when comparing results.

It is also worth discussing Patnaik et al.'s paper as the results achieved here are compared with their charging strategy. The temperatures and C-rate in both strategies are comparable and both studies are cooling the cells with convection. As such, the general results from Patnaik et al. can be compared to the results from the novel strategy; this should still be done with caution, however.

Finally, it should be noted that there is other interesting work currently taking place regarding charging strategies, namely using machine learning to generate an optimised profile for existing strategies such as MCC, (47), (to date, this is the only other work on closed-loop charging). The results of this study are promising, although the improvements are still comparable to those reported here. Some might suggest that this threatens the relevance of CT charging. This is not the case, however, and this method of optimisation could be applied to the CC-CT-CV strategy suggested here.

6.3 CC-CT-CV Improvements

Despite the disruptions, a complete and comprehensive set of results were still achieved. When compared to a CC-CV profile, the CC-CT-CV profile achieves a 7.4% reduction in charge time whilst simultaneously achieving a 28.7% reduction in ΔT, averaged over nearly 200 cycles. These results improve on Patnaik et al.'s CT-CV profile, showing a clear benefit to initially charging with CC. The CV stage takes significantly longer than in CC-CV, suggesting that reducing I_{max} could further improve the total charge time. The experimental results presented here validate the findings obtained computationally, which corroborated that a reduction in ΔT would be seen by using a CC-CT-CV strategy.

Despite a higher I_{max}, it is clear the novel CT profile results in less cell degradation then when a cell is cycled with CC-CV. A 24.8% reduction in capacity fade was measured after 200 cycles using OCV tests.

The predominate degradation mechanism encountered at this temperature would be SEI growth (26), which, as discussed in the literature review, contributes to the ohmic resistance, R_0. As SEI growth is directly proportional to temperature, any strategy reducing the maximum temperature which the cell is exposed to would reduce its growth. This theory is supported by the results presented here, with pulse testing showing that the ohmic resistance of the cell cycled with CC-CT-CV increased nearly half as much when compared to the control. The reduced growth of the SEI would also account for the reduction in capacity fade, with less active material, mainly Li^+, being consumed in its production.

These results constitute the *first* degradation study on the *first* CC-CT-CV based profile and provide a promising basis for work on this strategy to continue.

As aforementioned, no literature could be found which clearly categorises the peaks obtained from ICA for this particular cell chemistry. However, all papers which do discuss ICA show how the peaks move further from their BOL position the more they are cycled (33). While the comparison is qualitative rather than quantitative, Figure 24 clearly shows how all three major peaks have moved more for the cell cycled with CC-CV than for the cell cycled with the CT strategy. This implies that more degradation occurs within the cell cycled with CC-CV, further supporting the results of both pulse testing and the OCV tests. Should more research be done into ICA, then the IC curves presented in section 5 could be used to determine exactly which degradation mechanisms, or at least, which types, are being reduced by charging with a CT strategy.

Finally, the following research question was proposed in the introduction of this report:

Can constant-temperature charging strategies be further improved by introducing an initial CC stage to reduce the maximum current whilst maintaining the benefits in charge time?

Yes. As discussed above, the results obtained here suggest that adding a CC stage reduces the initial current without compromising on the reduction in ΔT and, in fact, could perhaps further reduce it.

6.4 Applications

Perhaps the most important aspect of this research is its ease of application. Given that the battery management system, BMS, onboard most EVs already communicates with the charging station (48), there would be no need for any additional hardware. CT charging strategies could potentially be applied to existing EVs, through existing charging stations, with the addition of merely a few lines of code.

Any applications of this research, however, would most likely depend on the interests of the company intending to use it and, in turn, the needs and demands of their customers. A 25% reduction in capacity fade could potentially equate to a similar increase in the lifespan of a battery pack, or a significant increase in charge time whilst keeping cycle life constant.

Whichever application is chosen, it is hoped that CT strategies, and more specifically, the CC-CT-CV strategy developed in this project, can be used to improve EVs and, in turn, help achieve net zero CO_2 emission targets.

7. Future Work

This project has provided crucial insight into CT charging strategies and has shown that this strategy could be significantly better for both cell life and charge time than the current industry standard. As alluded to in the introduction, a significant advantage of charging strategy technologies is that their benefits can be exploited rapidly; there is no need to wait for advancements in manufacturing and the technology could be applied to existing EVs with very little modification. Having said this, more work is needed to both validate these results and to produce an optimised CC-CT-CV profile.

It is hoped that the both the code and experimental work presented here will be published to the wider scientific community. This would encourage future work on CT strategies, and allow future researchers to model them with ease. It is also hoped that the author will continue to work on this project. The specifics of the work which needs to be completed next are outlined below.

First, a CT profile should be obtained using PID control. The results presented here should then be further validated. Whilst the cells were cycled nearly 200 times, meaning capacity fade and other degradation mechanisms were not simply measured over one cycle, the entire experiment should be repeated numerous times. This would allow a statistical significance to be calculated and would add further credibility to the results. Further, 200 cycles is not end of life for the cells, and they should be cycled until this occurs, perhaps 30% capacity fade, in case the trends shown here change towards end of life, (there is, however no good scientific reason why this should happen). Capacity fade should also be plotted against energy throughput rather than the number of cycles, so that the total charge passed through the cell will be identical, producing a more realistic comparison.

The degradation study could also be extended to include a GITT test to parameterise the ECN model and achieve more accurate results for the resistance change. The ICA could be conducted using the LEAN approach, (34), to remove the filtering issues, and additional research could be conducted to categorise the peaks seen in the IC plots.

Once this work is completed, an optimum CC-CT-CV profile should be found. This should be done for a range of different ambient temperatures as the results will vary. For example, if the at rest temperature is 30°C, charging a CT set at 31°C may be too slow, however if the ambient temperature is 25°C, as it was in this experiment, 31°C would be unnecessarily high and may not be reached in the CC stage.

An ideal future application based on this work would be one where the owner of an EV could select the required charge time, and a program will charge the battery pack with the optimised CT strategy by varying I_{max} and T_{max} accordingly.

8. Conclusions

The aims of this project were to advance research on closed-loop charging strategies and to develop a CT based strategy which outperforms existing solutions.

Functions were written to allow the MATLAB based model 'LIONSIMBA' to run CT strategies and was used to develop a CC-CT-CV strategy. The particular profile developed could theoretically match the reduction in ΔT shown by the only existing CT strategy, without relying on a large input current. This has promising implications for temperature dependant degradation mechanisms, particularly SEI growth.

The project had a strong focus on applications in the EV industry, with the cells used in experimentation, LG M50 21700, selected to reflect this. With the necessary hardware unavailable, PID control could not be used to develop a CT profile. In its place, a quasi-CT profile was produced using the software linked to the testing unit, the Maccor.

The key results of this CC-CT-CV profile are provided below when compared to a CC-CV control.

- 7.4% reduction in charge time
- 28.7% reduction in temperature rise
- The percentage increase in I_{max} was almost four times less than existing CT strategies

Cycling tests, accompanied by characterisation tests, were carried out on two 21700s, one cycling with CC-CV, and another with the CC-CT-CV profile. After 200 cycles, when compared with the CC-CV control, the cell cycled with CC-CT-CV showed:

- 24.8% reduction in capacity fade
- 45.0% reduction in the increase in ohmic resistance

These results show how charging with CC-CT-CV causes less degradation, most likely SEI growth, whilst simultaneously outperforming CC-CV in terms of charge time.

With these promising results, it is hoped that the work on CT charging strategies, specifically CC-CT-CV, will continue to be built upon, and may one day be used to charge commercial EVs.

9. References

(1) Patnaik L, Praneeth, A. V. J. S, Williamson SS. A Closed-Loop Constant-Temperature Constant-Voltage Charging Technique to Reduce Charge Time of Lithium-Ion Batteries. *IEEE Transactions on Industrial Electronics*. 2019; 66 (2): 1059-1067. Available from: doi: 10.1109/TIE.2018.2833038

(2) *To What Extent Can Charging Strategies be Used to Aid the Development of Fast Charging in Electric Vehicles?* Internal Unpublished Article; 2018.

(3) IEA. Tracking Clean Energy Progress 2017. 2017; Available from: https://webstore.iea.org/download/direct/301

(4) Sager J, Apte JS, Lemoine DM, Kammen DM. Reduce growth rate of light-duty vehicle travel to meet 2050 global climate goals. *Environmental Research Letters*. 2011; 6 (2): 024018. Available from: doi: 10.1088/1748-9326/6/2/024018

(5) Contestabile M, Offer GJ, Slade R, Jaeger F, Thoennes M. Battery electric vehicles, hydrogen fuel cells and biofuels. Which will be the winner? *Energy & Environmental Science*. 2011; 4 (10): 3754-3772. Available from: doi: 10.1039/c1ee01804c

(6) Ferguson CR. *Internal combustion engines: applied thermosciences*. Third edition; 2016.

(7) *New & Used Electric Cars | Tesla UK*. Available from: https://www.tesla.com/en_GB/inventory/new/ms

(8) Reynolds J. FYP - Experimental Assessment of Fast Charging Techniques in Lithium Ion Batteries - Project Plan. Internal Unpublished Article; November 7, 2019.

(9) Hirano H, Tajima T, Hasegawa T, Sekiguchi T, Uchino M. Boiling Liquid Battery Cooling for Electric Vehicle. *2014 IEEE Conference and Expo Transportation Electrification Asia-Pacific (ITEC Asia-Pacific)*: IEEE; Aug 2014. pp. 1-4. Available from: 10.1109/ITEC-AP.2014.6940931.

(10) Hunt IA, Zhao Y, Patel Y, Offer J. Surface Cooling Causes Accelerated Degradation Compared to Tab Cooling for Lithium-Ion Pouch Cells. *Journal of The Electrochemical Society*. 2016; 163 (9): A1846-A1852. Available from: doi: 10.1149/2.0361609jes

(11) Agrawal RC, Pandey GP. Solid polymer electrolytes: materials designing and all-solid-state battery applications: an overview. *Journal of Physics D: Applied Physics*. 2008; 41 (22): 223001. Available from: doi: 10.1088/0022-3727/41/22/223001

(12) Kahn J. *Inside James Dyson's Costly Decision to Kill His Electric Car*. Available from: https://fortune.com/longform/james-dyson-electric-car-appliances/

(13) Reynolds J. FYP - Experimental Assessment of Fast Charging Techniques in Lithium Ion Batteries - Progress Report. Internal Unpublished Article; Jan 31, 2020.

(14) Reddy TB, Linden D, Linden D. *Linden's handbook of batteries*. 4th ed. New York; London: McGraw-Hill; 2011.

(15) Wu B, Merla Y, Yufit V, Brandon NP, Martinez-Botas R, Offer GJ. *Novel application of differential thermal voltammetry as an in-depth state-of-health diagnosis method for lithium-ion batteries.* Elsevier; 2016.

(16) Schindler S, Bauer M, Cheetamun H, Danzer MA. Fast charging of lithium-ion cells: Identification of aging-minimal current profiles using a design of experiment approach and a mechanistic degradation analysis. *Journal of Energy Storage.* 2018; 19 364-378. Available from: doi: 10.1016/j.est.2018.08.002

(17) Zhang SS. The effect of the charging protocol on the cycle life of a Li-ion battery. *Journal of Power Sources.* 2006; 161 (2): 1385-1391. Available from: doi: 10.1016/j.jpowsour.2006.06.040

(18) Remmlinger J, Tippmann S, Buchholz M, Dietmayer K. Low-temperature charging of lithium-ion cells Part II: Model reduction and application. *Journal of Power Sources.* 2014; 254 268-276. Available from: doi: 10.1016/j.jpowsour.2013.12.101

(19) Doyle M. Modeling of Galvanostatic Charge and Discharge of the Lithium/Polymer/Insertion Cell. *Journal of The Electrochemical Society.* 1993; 140 (6): 1526. Available from: doi: 10.1149/1.2221597

(20) Ge H, Aoki T, Ikeda N, Suga S, Isobe T, Li Z, et al. Investigating lithium plating in lithium-ion batteries at low temperatures using electrochemical model with NMR assisted parameterization. *Journal of the Electrochemical Society.* 2017; 164 (6): A1050-A1060. Available from: doi: 10.1149/2.0461706jes

(21) Vetter J, Novák P, Wagner MR, Veit C, Möller K-, Besenhard JO, et al. Ageing mechanisms in lithium-ion batteries. *Journal of Power Sources.* 2005; 147 (1-2): 269-281. Available from: doi: 10.1016/j.jpowsour.2005.01.006

(22) Pinson MB, Bazant MZ. Theory of SEI Formation in Rechargeable Batteries: Capacity Fade, Accelerated Aging and Lifetime Prediction. *Journal of the Electrochemical Society.* 2013; 160 (2): A243-A250. Available from: doi: 10.1149/2.044302jes .

(23) Liu Q, Du C, Shen B, Zuo P, Cheng X, Ma Y, et al. Understanding undesirable anode lithium plating issues in lithium-ion batteries. *RSC Advances.* 2016; 6 (91): 88683-887. Available from: doi: 10.1039/c6ra19482f .

(24) Anseán D, González M, Viera JC, García VM, Blanco C, Valledor M. Fast charging technique for high power lithium iron phosphate batteries: A cycle life analysis. *Journal of Power Sources.* 2013; 239 9-15. Available from: doi: 10.1016/j.jpowsour.2013.03.044

(25) Pinson MB, Bazant MZ. *Theory of SEI Formation in Rechargeable Batteries: Capacity Fade, Accelerated Aging and Lifetime Prediction.* 2012.

(26) Vetter J, Novák P, Wagner MR, Veit C, Möller K-, Besenhard JO, et al. Ageing mechanisms in lithium-ion batteries. *Journal of Power Sources.* 2005; 147 (1): 269-281. Available from: doi: 10.1016/j.jpowsour.2005.01.006

(27) Offer G, Marinescu M. Future Clean Transport Technology - Battery cell ageing and degradation. Internal Unpublished Article; 2020.

(28) Harks, P. P. R. M. L., Mulder FM, Notten PHL. In situ methods for Li-ion battery research: A review of recent developments. *Journal of Power Sources*. 2015; 288 92-105. Available from: doi: 10.1016/j.jpowsour.2015.04.084

(29) Hussein AA. Capacity Fade Estimation in Electric Vehicle Li-Ion Batteries Using Artificial Neural Networks. *IEEE Transactions on Industry Applications*. 2015; 51 (3): 2321-2330. Available from: doi: 10.1109/TIA.2014.2365152

(30) Bergamaschi L, Bumharter C, Pollock C, Reynolds J, Wild J. FCTT - Modelling Li-ion Batteries to Understand Limitations of Performance. Internal Unpublished Article; Mar 13, 2020.

(31) Jackey R, Saginaw M, Sanghvi P, Gazzarri J, Huria T, Ceraolo M. *Battery Model Parameter Estimation Using a Layered Technique: An Example Using a Lithium Iron Phosphate Cell*. 2013.

(32) Weng C, Feng X, Sun J, Peng H. State-of-health monitoring of lithium-ion battery modules and packs via incremental capacity peak tracking. *Applied Energy*. 2016; 180 360-368. Available from: doi: 10.1016/j.apenergy.2016.07.126

(33) Dubarry M, Truchot C, Liaw BY. Synthesize battery degradation modes via a diagnostic and prognostic model. *Journal of Power Sources*. 2012; 219 204-216. Available from: doi: 10.1016/j.jpowsour.2012.07.016

(34) Feng X, Merla Y, Weng C, Ouyang M, He X, Liaw BY, et al. A reliable approach of differentiating discrete sampled-data for battery diagnosis. *eTransportation*. 2020; 3 Available from: doi: 10.1016/j.etran.2020.100051

(35) Jeon DH, Baek SM. Thermal modeling of cylindrical lithium ion battery during discharge cycle. *Energy Conversion and Management*. 2011; 52 (8-9): 2973-2981. Available from: doi: 10.1016/j.enconman.2011.04.013

(36) Mao-de Li, Wang F. *Thermal Performance Analysis of the Lithium-Ion Batteries*. 2010.

(37) Bernardi D. A General Energy Balance for Battery Systems. *Journal of the Electrochemical Society*. 1985; 132 (1): 5. Available from: doi: 10.1149/1.2113792

(38) Amietszajew T, Mcturk E, Fleming J, Bhagat R. Understanding the limits of rapid charging using instrumented commercial 18650 high-energy Li-ion cells. *Electrochimica Acta*. 2018; 263 346-352. Available from: doi: 10.1016/j.electacta.2018.01.076

(39) Abousleiman R, Al-Refai A, Rawashdeh O. *Charge Capacity Versus Charge Time in CC-CV and Pulse Charging of Li-Ion Batteries*. 2013.

(40) Li S, Zhang C, Xie S. Research on fast charge method for lead-acid electric vehicle batteries. *2009 International Workshop on Intelligent Systems and Applications, ISA 2009, May 23, 2009 - May 24, 2009*. Wuhan, China: IEEE Computer Society; 2009. pp. Huazhong Normal University; Huazhong University of Science and Technology; Hubei University of Technology; IEEE Harbin Section. Available from: 10.1109/IWISA.2009.5073068

(41) Tomaszewska A, Chu Z, Feng X, O'Kane S, Liu X, Chen J, et al. *Lithium-ion battery fast charging: A review*. Elsevier; 2019.

(42) Lyu Y, Siddique ARM, Majid SH, Biglarbegian M, Gadsden SA, Mahmud S. Electric vehicle battery thermal management system with thermoelectric cooling. *Energy Reports*. 2019; 5 822-827. Available from: doi: 10.1016/j.egyr.2019.06.016

(43) Torchio M, Magni L, Gopaluni RB, Braatz RD, Raimondo DM. LIONSIMBA: A Matlab Framework Based on a Finite Volume Model Suitable for Li-Ion Battery Design, Simulation, and Control. *Journal of the Electrochemical Society*. 2016; 163 (7): A1192-A1205. Available from: doi: 10.1149/2.0291607jes

(44) Rydh CJ, Sandén BA. Energy analysis of batteries in photovoltaic systems. Part I: Performance and energy requirements. *Energy Conversion and Management*. 2005; 46 (11): 1957-1979. Available from: doi: 10.1016/j.enconman.2004.10.003

(45) Tomaszewska A, Chu Z, Feng X, O'Kane S, Liu X, Chen J, et al. Lithium-ion battery fast charging: A review. *eTransportation*. 2019; 1 100011. Available from: doi: 10.1016/j.etran.2019.100011

(46) Love J. *PID Control*. London; 2007.

(47) Attia PM, Grover A, Jin N, Severson KA, Markov TM, Liao Y, et al. Closed-loop optimization of fast-charging protocols for batteries with machine learning. 2020.

(48) Pecht M, Tsui KL, Xing Y, Eden WMM. Battery Management Systems in Electric and Hybrid Vehicles. *Energies*. 2011; 4 (11): 1840-1857. Available from: doi: 10.3390/en4111840